A Hedonic Social Cost of Carbon: Evidence from US Migration*

Tamma Carleton† Marco Tabellini‡ Charles A. Taylor§ Guglielmo Zappalà¶

March 2026

Preliminary: Please do not cite or circulate

Abstract

This paper proposes a novel empirical approach to estimating the costs of climate change by examining how migrants trade off a change in their long-run climate against real income. Migration events often involve a shift in a migrant's climatology that is comparable in magnitude to warming projections over the 21st century. Assuming that migrants know how these climatic differences affect their economic and social well-being, we combine U.S. Census data on individual migration decisions, labor market outcomes, housing costs, and demographic characteristics into a discrete choice framework to assess how potential earnings and climate jointly influence relocation decisions within the United States. We use these estimates to infer a willingness-to-accept value for climate change, demonstrating robustness to myriad modeling approaches. We examine how this revealed preference for avoiding climate change differs by age, gender, and other demographics. We then combine these valuation estimates with a global simple climate model and probabilistic future projections of emissions and socioeconomic change to compute a social cost of carbon (SCC) for the U.S., contributing a new method for SCC estimation to a growing body of research aiming to quantify the costs of a warming world.

*We are grateful to Joe Aldy, Kirill Borusyak, Gabriel Kreindler, Eliana La Ferrara, Ishan Nath, Anna Russo, Wolfram Schlenker, Ben Sprung-Keyser, Jim Stock, and participants at ASSA 2026, MIT/Harvard seminar for helpful suggestions and comments. Sherry Tang provided excellent research assistance.

†Department of Agricultural and Resource Economics, UC Berkeley, and NBER.

‡Harvard Business School, NBER, CEPR, and LISER.

§Harvard Kennedy School, and NBER.

¶Harvard University, Center for the Environment.

1 Introduction

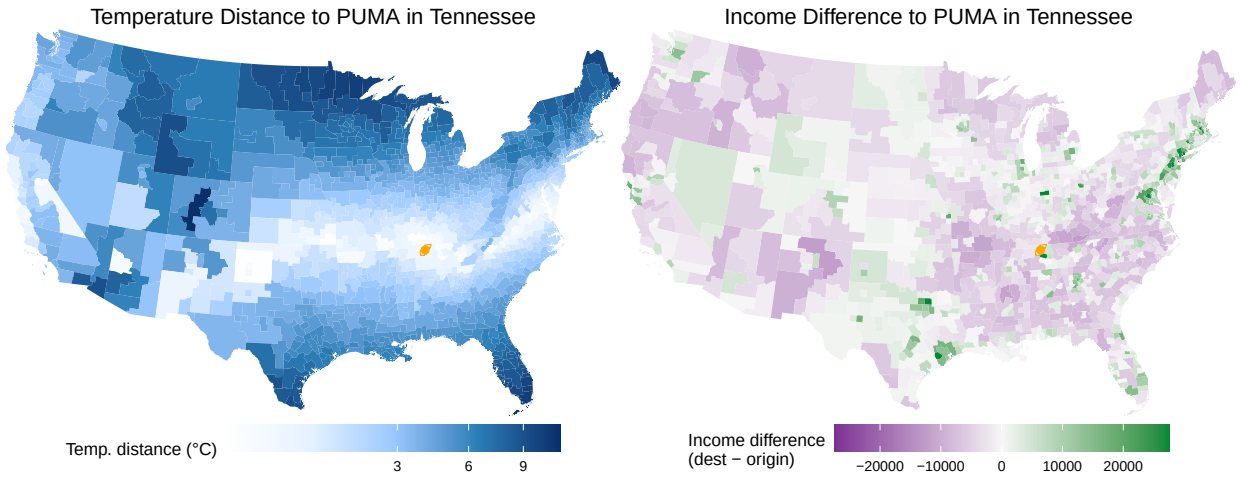
Estimates of the economic burden of climate change remain uncertain, varying widely across methodologies and study contexts. Moreover, while direct effects on economic output or human health tend to be empirically tractable, the plausibly large but difficult-to-measure amenity value of the climate remains particularly elusive. In an ideal experiment, a researcher would perturb the climate of several otherwise identical worlds and observe the divergence in long-run economic outcomes. This would allow for a direct mapping of permanent shifts in temperature distributions to economic production.

We propose an alternative approach: using human migration as a laboratory for climate change. By definition, a migrant moves from one climate state to another. In so doing, she trades off a change in her climate against the economic opportunities afforded by the move, revealing her willingness to accept this shift in climatological conditions. For example, the left panel in Figure 1 shows the absolute value of the change in long-run average temperature experienced by a migrant leaving Nashville, Tennessee, for any other region of the continental U.S. In choosing a potential destination, this same migrant simultaneously evaluates her economic opportunities, shown in the right panel as the difference in average income between all potential destinations and her home location of Nashville. For example, a horizontal move to northern Arkansas would allow her to maintain a very similar climate, but would lower her expected income. In contrast, a move to New England would substantially increase economic opportunity, but dramatically change her climatology, presenting a climate-income tradeoff in her migration decision.

We exploit these tradeoffs to estimate a model of location choice, recovering migrants' willingness to accept deviations from their specific climate niche. Using U.S. Census data from 2000 to 2016 on individual migration decisions, labor market outcomes, housing costs, and demographic characteristics, we estimate a gravity model (Anderson and Van Wincoop 2003) of bilateral migration flows across roughly 1,000 Public Use Microdata Areas (PUMAs). The model includes origin-by-period fixed effects, which absorb all time-varying characteristics of the origin, and destination fixed effects, which absorb time-invariant destination attributes—including amenities, climate levels, and other location fundamentals. The temperature distance coefficient is therefore identified from variation across origins sending migrants to the same destination: among all origins, those climatically closer send disproportionately more migrants, conditional on income and demographics.

Consistent with established labor literature, we observe that migrants move toward higher real incomes. According to our estimates, a 10% increase in income in the destination

Figure 1: Migration as a revealed preference for climate change



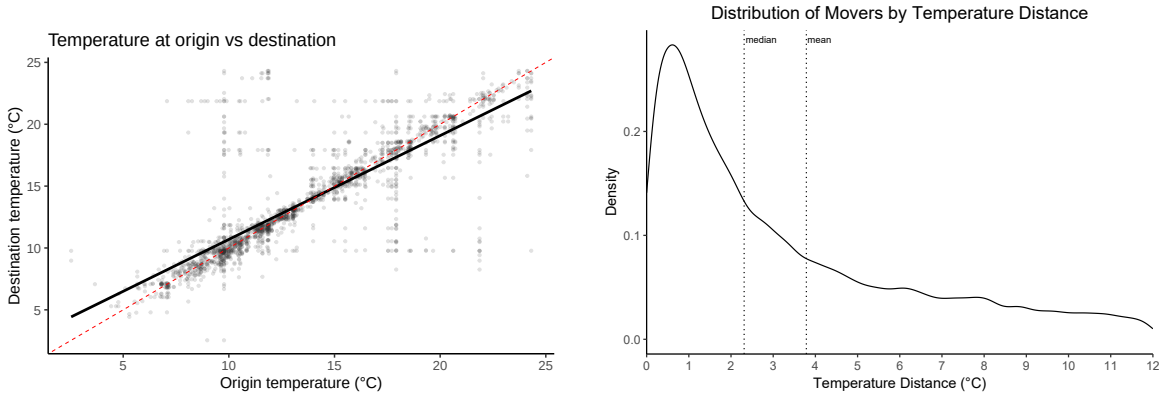
Note: Figures show Public Use Microdata Areas (PUMAs) across the United States. Left panel shows the absolute value of the difference in long-run average temperature between each PUMA and Nashville, Tennessee (measured in degrees Celsius from the TerraClimate dataset). Right panel shows the difference in average annual income (adjusted for housing costs) between each PUMA and Nashville (measured in 2020 USD). See Section 3.1 for details on data.

increases migration by 4.7%, in line with prior literature (Kennan and Walker 2011). However, they also avoid destinations with significant climatological differences—measured by temperature and precipitation differentials—relative to their origin. This mirrors findings by Obolensky et al. 2024, who document that migrants seek to minimize climate distance in various historical settings. In our context, increasing temperature distance by 1°C reduces migration by 5.7%, indicating a sizable revealed-preference penalty for moving outside one's climatic equilibrium. Indeed, Figure 2 (left panel) shows that a positive correlation between origin and destination temperature is apparent in the raw data we assemble for the modern U.S. Together, the coefficients linking income to migration and linking temperature distance to migration enable us to compute the marginal rate of substitution between income and climate change, revealing migrants' willingness to accept a change in climate in exchange for real income. We find that, on average, household heads are willing to accept $4,742 in additional annual income to move 1°C from their long-run equilibrium climate.

We additionally show that willingness-to-accept valuations are similar across genders, but systematically decline with age. Figure 2 (right panel) shows that the average mover experiences a magnitude of climate change (3.8°C) that is comparable to projected future warming, making these estimates empirically relevant to the valuation of long-run climate change.

This specification implies that any change from a migrant's origin climate is costly. A

Figure 2: Climate matching in internal U.S. migration



Note: Left panel shows the long-run average temperature in degrees Celsius for each Public Use Microdata Area (PUMA) "origin" (x-axis) and each PUMA "destination" (y-axis) for the largest 2,000 internal migratory flows in the United States in our estimation sample (years 2000–2016). The positive correlation indicates migrants' preference for matching climates across origin and destination locations. Right panel plots the distribution of total migrants for all PUMA pairs by the temperature distance between each pair of localities. See Section 3.1 for details on data.

natural question is whether this interpretation is consistent with widely documented Sunbelt migration trends in the United States (Glaeser and Tobio 2008). In our sample, movers relocate to destinations that are on average 0.44°C warmer than their origin locality, with New York to Florida constituting the single largest interstate migration corridor. A map of net migration flows (Figure A1) confirms that net receivers cluster in the South and Southwest. These patterns reflect the well-known pull of Sunbelt destinations, driven by job growth, lower housing costs, favorable taxes, and retirement and elder-care infrastructure—all of which are appealing independent of a preference for warmth. We show that once the general attractiveness of warm destinations is accounted for, what remains is a robust symmetric climate distance penalty. That is, when comparing among *all* origins sending migrants to the *same* destination, we find that those from climatically similar locations send disproportionately more, conditional on income, demographics, and a suite of nonparametric controls.

Our "migration as a laboratory" approach offers three distinct advantages. First, we exploit relative *changes* in climate between a migrant's origin and destination. This helps mitigate many of the identification concerns that threaten a causal interpretation of results from prior literature studying the value of climate amenities across space (Albouy et al. 2016; Mathes 2025; Sinha et al. 2018; Timmins 2007). Second, we show that this specification relying on temperature "distance" uncovers the costs of *adapting* to a new long-run climate equilibrium. It is increasingly clear that people and economies adapt to their local climates (Carleton et

al. 2022; Heutel et al. 2021), making adaptation costs a critical component of aggregate damages from climate change (Lemoine 2018; Mendelsohn et al. 1994). Yet measuring such adaptation costs is notoriously difficult, as there are many margins of adaptation and enumerating each, as well as their monetary value, is infeasible. Our revealed preference estimates uncover the total costs of adapting to a new long-run climate equilibrium without needing to enumerate specifically how individuals, firms, and governments adapt. Finally, our estimates include both market and non-market (e.g., amenity) channels through which climate change can influence well-being, while much prior work focuses on one (Burke et al. 2015) or the other (Carleton et al. 2022), and most fail to capture pure amenity values.

We address identification and selection concerns through several robustness checks. For example, to address spatial correlation in climate, we control for road-network travel time—which is less correlated with climate gradients than geodesic distance—and we also show robustness to excluding short-distance and within-state moves. To account for the endogeneity of destination income, we instrument for income using a Bartik industry shock (Bartik 1991) and the China shock (Autor et al. 2013). We show that our results are robust to model choice (PPML versus OLS), exploiting panel versus cross-sectional variation, leaving one state out, and using an instrument for income. Our results are robust to controlling for established migrant networks and alternative measures of climate "distance."

Using these estimates, we calculate a Social Cost of Carbon (SCC) for the United States representing the aggregate costs of adapting to the warming caused by a marginal ton of CO_2. To do so, we leverage a probabilistic global climate model to perturb the global climate with a pulse of CO_2 and compute the present discounted value of the stream of resulting damages, which are valued using our willingness-to-pay estimates. We show that the SCC we recover—approximately \$56 for the United States—is similar to, but slightly larger than, values in the recent climate economics literature, including models used by the Biden administration in a 2023 update of the SCC.[1] Our damage estimate is also larger than the \$15 comprehensive carbon price for the United States in 2019 (Carhart et al. 2022). This weighted-average metric aggregates the marginal incentives to reduce CO_2 emissions across a country's entire policy mix, including emissions trading systems, fossil fuel taxes and subsidies, renewable energy mandates, and fuel standards.

Our approach to estimating a domestic SCC is relevant for U.S. policy in light of regulatory mandates (OMB Circular A-4) to monetize domestic benefits. Unlike Integrated Assessment

[1] Our domestic SCC of \$56 is higher than the domestic damages calculated by the DSCIM (\$21), GIVE (\$24), and FREDI (\$36) models (Kopits et al. 2025). These estimates are distinct and complementary: while prior models primarily aggregate sector-specific physical damages, our revealed preference approach captures the amenity and productivity costs of adjusting to a new long-run climate equilibrium.

Models that rely on downscaling a global SCC to estimate national damages, our approach constructs a U.S.-specific value from the bottom up using domestic migration decisions. In future work, our approach could be applied in other countries to aggregate bottom-up estimates of the global SCC.

The paper is organized as follows. Section 2 presents our conceptual model, from which we derive our empirical estimating equation. Section 3 describes our data and empirical strategy, while Section 4 presents empirical results. In Section 5 we use these results to compute a U.S. social cost of carbon.

2 Conceptual model

We use a standard residential sorting model to derive estimating equations that link migration decisions, income, and changes in climate. Intuitively, we recover willingness to pay for changes in the climate by estimating how individual migrants trade off earnings in a potential destination with the climate difference between their origin and that destination. The degree to which migrants are willing to sacrifice climate similarity for income reveals their willingness to accept a change in the climate.

Specifically, we follow prior literature that uses migration to infer the value of environmental amenities (Bayer et al. 2009; Freeman et al. 2019) and develop a static residential sorting model with nonlinear utility. We assume household i chooses location j along with consumption of a composite commodity $C_{i,j}$ and housing services $H_{i,j}$ to maximize its utility subject to a budget constraint:

$$\max_{C_{i,j},H_{i,j}} U(C_{i,j}, H_{i,j}, \Delta T_{i,j}) \quad \text{s.t.} \quad C_{i,j} + r_j H_{i,j} = I_j \tag{1}$$

where I_j is household income in location j, r_j represents the unit price of housing services in location j, and $\Delta T_{i,j} = |T_j - T_i|$ is the absolute value of the temperature difference between household i's origin and its current residence j.[2] This temperature specification implicitly assumes that agents adapt to their long-run climate, such that temperature *differences* between origin and destination reduce utility. This structure is motivated by our own findings (Figure 2) and those of prior work (Obolensky et al. 2024)) showing that higher temperature differences lower migrants' propensity to move.

[2] We note that this slight abuse of notation, in which i indexes both the household and its origin location, is for parsimony only. All expressions would follow similarly if we indexed households and origins separately.

To gain traction empirically, we specify the structure of the utility function for household i residing in location j as:

$$U_{i,j} = C_{i,j}^{\beta_C} H_{i,j}^{\beta_H} \exp[M_{i,j} + \beta_{\Delta T} \Delta T_{i,j} + \eta_{i,j}] \tag{2}$$

where $\eta_{i,j}$ is a household-specific idiosyncratic term that is independent of location attributes and of $M_{i,j}$, the utility cost of moving from origin climate T_i to destination climate T_j. Household utility maximization yields the optimal consumption of housing services:

$$H_{i,j}^* = \frac{\beta_H}{\beta_H + \beta_C} \frac{I_{i,j}}{r_j} \tag{3}$$

Substituting $H_{i,j}^*$ for $H_{i,j}$ in Equation (2) and using the budget constraint yields the following household indirect utility function:

$$V_{i,j} = A \exp[\beta_I \ln I_{i,j} - \beta_H \ln r_j + \beta_{\Delta T} \Delta T_{i,j} + M_{i,j} + \eta_{i,j}], \tag{4}$$

where $A = \beta_H^{\beta_H} \beta_C^{\beta_C} / (\beta_H + \beta_C)^{(\beta_H + \beta_C)}$ is a constant that drops out of the discrete choice problem and $\beta_I = \beta_H + \beta_C$. The marginal willingness to pay (MWTP) for a change in climate is thus the marginal rate of substitution between $\Delta T_{i,j}$ and household income:

$$MWTP_{\Delta T_{i,j}} = \frac{\beta_{\Delta T}}{\beta_I} I_{i,j} \tag{5}$$

If we take logs of Equation (4) and assume the unobservable error terms η_{ij} are independently and identically distributed across individuals and locations type I extreme value (standard Gumbel), and that individuals i choose the location j that maximizes utility, as specified in Equation (2), the probability that i chooses j from the set of possible choices J is:

$$\begin{aligned} \pi_{i,j} &= Pr(\ln V_{i,j} > \ln V_{i,\ell} \, \forall \ell \neq j) \\ &= \frac{\exp[\beta_I \ln I_{i,j} - \beta_H \ln r_j + \beta_{\Delta T} \Delta T_{i,j} + M_{i,j}]}{\sum_{\ell \in J} \exp[\beta_I \ln I_{i,\ell} - \beta_H \ln r_\ell + \beta_{\Delta T} \Delta T_{i,\ell} + M_{i,\ell}]} \end{aligned} \tag{6}$$

In Section 3.2, we describe our empirical strategy to use Equation (6) to recover coefficients $\beta_{\Delta T}$ and β_I using maximum likelihood. These estimates are then used to construct an

estimate of the marginal willingness to pay following Equation (5).

3 Data and empirical strategy

3.1 Data

Our analysis relies primarily on a custom harmonization of U.S. census data migration records over four waves. We combine these records of individual-level origin and destination pairings with climatological data, housing data from the Integrated Public Use Microdata Series (IPUMS), and travel time data from Open Street Map. Here we describe each data source and our process of harmonization.

3.1.1 Census data

We use publicly-available information from the U.S. Census years 2000, 2006, 2011, 2016, obtained from both IPUMS and the American Community Survey (ACS), depending on the year. Observations are at the individual level and contain the location of residence at the scale of a Public Use Microdata Area (`PUMA`) (`PUMA`s are geographic areas containing between 100,000 to 200,000 people). Each observation additionally indicates the location where the person last lived either 5 years ago (year 2000 data) or 1 year ago (all other years). Birthplace locations are recorded at the spatial resolution of a U.S. state or country. Additional relevant covariates obtained from these census data include income, housing costs (rental rate or housing value), and demographic information, such as age, sex, number of children, and education level. To estimate after-tax income, we use the NBER TAXSIM model to adjust for state taxes (more details can be found in Appendix E). For regressions estimated using instrumental variables, we used the Census employment records and constructed local industry composition variables. To make industry composition comparable across years, we used the `IND1990` classification for every year and assigned each individual to an industry based on the `IND1990` value. For the purpose of our current analysis, we limit our sample to heads of households only.

3.1.2 Data aggregation

While our raw data are at the `PUMA` level, our unit of analysis is the Migration Public Use Microdata Area (known as the `MIGPUMA`). Using `MIGPUMA` enables us to construct a constant

geography over time, as PUMA boundaries and migration coding change temporally. Thus, we harmonize geographies across census and ACS samples using IPUMS-generated crosswalks from PUMAs to migration PUMAs. As `MIGPUMA` is higher resolution, we use this level as our estimating sample.

To implement this, for each cross-sectional census year ($t \in \{2000, 2006, 2011, 2016\}$), we construct origin and destination identifiers at the `MIGPUMA` level. We define the destination j as the respondent's current `PUMA`, mapped to a `MIGPUMA` using the official crosswalks between `PUMA` and `MIGPUMA` provided by `IPUMS`. We then form a national key by concatenating the state FIPS and the `MIGPUMA` codes. Origins i are defined from the IPUMS migration variables (previous `MIGPUMA`), again restricted to domestic U.S. states and mapped to the same national `MIGPUMA` key. To keep stayers in the sample, observations with missing origin codes are assigned $i = j$.

At the individual level we retain annual income and standard demographic characteristics. As detailed below, we estimate regressions at the origin-destination level, collapsing all place-based covariates to the i (origin) or j (destination) level using Census person weights (`PERWT`). For example, to compute destination income, we calculate population-weighted average income across all residents (both arrivals and stayers). This process yields resident means of income, housing costs, housing tenure, education, and other demographics at the `MIGPUMA` level. We then merge in climate variables computed for each `MIGPUMA`, and attach to each origin i and each destination j in the migration data.

The resulting person-level dataset for each cross section contains (i, j) identifiers, individual income and housing costs, and origin and destination place-level variables such as mean income, mean housing costs, mean covariates such as education and race, and local climate. From this microdata we construct origin–destination migratory flow matrices by summing person weights within each (i, j) cell. We then expand each cross-section to the full Cartesian product of observed origins and destinations, assigning zero flows to unobserved (i, j) pairs and merging in the corresponding origin and destination characteristics. These expanded $i - j$ panels form the basis of our regressions. In our main analysis, we limit moves to those over 80km to capture moves outside local labor markets (Internal Revenue Service 2023; Johnson and Kleiner 2020), but we show robustness to alternative cutoffs as well.

In some additional analysis, we report heterogeneous willingness to pay estimates by demographic demographic group c (e.g., male vs. female, age<65 vs. 65+, college vs. no college, and ethnicity groups). We refer to these groups as "folds." For each fold c and cross-section t we compute: (i) the weighted number of movers n_{ijc} between each origin–destination pair,

and (ii) fold-specific resident means of income, housing costs, and covariates at origin and destination. We again expand to the full $i \times j \times c$ grid, so the estimation sample includes all potential moves (with zero flows where no migration is observed) with consistent origin, destination, and fold-specific covariates.

More details about the data aggregation can be found in Appendix B.

3.1.3 Constructing real income estimates

To identify the role of income in shaping migration decisions while accounting for large differences in costs of living across the U.S., we follow prior work in defining *real income* as nominal income net of housing expenditure. For each household i in location j and census year t, let y_{ijt} denote total annual income, reported directly from IPUMS. Additionally, IPUMS reports housing tenure (rent versus own), the monthly contracted rent, and self-reported housing value.[3] Housing expenditure depends on tenure. For renters, we set annual housing cost equal to twelve times monthly rent,

$$C_{ijt}^{R} = 12 \times rent_{ijt}.$$

For homeowners, we impute an annual "rental equivalent" using a user-cost measure. Specifically, we compute an after-tax user-cost rate UC_{ijt} and define the annual housing cost C_{ijt}^{O} as

$$C_{ijt}^{O} \equiv H_{ijt}\, UC_{ijt},$$

where H_{ijt} is the reported house market value. We follow the housing user-cost literature (Poterba 1984; Himmelberg et al. 2005; Wrenn 2024) to specify the after-tax user-cost rate for household i in location j and year t as:

$$UC_{ijt} = r_t^f + (1 - \tau_{ijt})\, \omega_{jt} + \mathbb{1}_{\text{mort},ijt}\, (1 - \tau_{ijt})\, r_t^m + \delta - \text{appr}_j. \tag{7}$$

Here, r_t^f is the nominal risk-free rate (10-year Treasury yield), r_t^m is the 30-year fixed mortgage rate, ω_{jt} is the local property tax rate, τ_{ijt} is the household's federal marginal income tax rate, $\mathbb{1}_{\text{mort},ijt}$ is an indicator for having a mortgage, δ is the economic depreciation and maintenance rate, and appr_j is the expected capital-gains rate on housing in state j. In our baseline, we fix $\delta = 0.025$ and allow the other components to vary across time, locations,

[3] We extract the variables `INCTOT`, `OWNERSHP`, `RENT`, and `VALUEH` from IPUMS for total annual income, housing tenure, contracted rent, and housing value, respectively. We drop top-coded values (coded as 9,999,999) and treat zero rents as missing.

and households. More details about housing cost calculation can be found in Appendix C.

Our preferred measure of real income is then:

$$I_{ijt}^{\text{net}} = I_{ijt} - C_{ijt},$$

where $C_{ijt} = C_{ijt}^{R}$ for renters and $C_{ijt} = C_{ijt}^{O}$ for homeowners.

3.1.4 Climate data

Climate data come from the TerraClimate global atmospheric reanalysis product and aggregated to the Migration Public Use Microdata Area (MIGPUMA) level. We calculate population-weighted climate averages using gridded population data from the HYDE 3.2 (Klein Goldewijk et al. 2017). For each geography, we construct long-run climatological normals from 1960–2000. The main variables of interest are mean annual temperature and precipitation, but we also compute seasonal averages for additional analysis.

3.1.5 Additional data sources

We measure bilateral travel costs using network-based driving distance and time derived from OpenStreetMap. Specifically, for each MIGPUMA, we construct a representative location given by the population-weighted centroid of residential coordinates. We then compute pairwise driving costs between all origin–destination pairs using the Open Source Routing Machine (OSRM) with the car routing profile and the publicly hosted OSRM server, which routes over the OpenStreetMap road network. That is, we submit the full set of MIGPUMA centroids to the OSRM table API and obtain the length (in kilometers) and duration (in minutes) of the fastest available road route between the origin and the destination, which reflects actual connectivity (including highways, local roads, and major bridges) rather than physical distance. We merge these bilateral driving distance and time measures back to the main dataset and use them as controls.

To address potential endogeneity of income, we construct a measure of exposure to the growth of Chinese import competition. The import data we use is from Autor et al. 2013. More details about the China shock construction can be found in Appendix D.

Similarly, to address the potential influence of past migration networks on migration choice, we add the number of historic migrants between the origin and the destination as control, using the 1850-1940 internal migration data from Obolensky et al. 2024 and collapsing their

data from county level into the MIGPUMA level.

3.2 Estimation

As described above in Section 2, we obtain migration probabilities by aggregating over individuals using the assumption that unobservable errors $\eta_{i,j}$ are distributed following a standard Gumbel distribution. This gives us closed form migration flows from Equation (6). We can then write that the share of migrants from i to j is equal to:

$$\pi_{ij} = \frac{\exp[\beta_I \ln I_{i,j} - \beta_H \ln r_j + \beta_{\Delta T} \Delta T_{i,j} + M_{i,j}]}{\sum_{\ell \in J} \exp[\beta_I \ln I_{i,\ell} - \beta_H \ln r_\ell + \beta_{\Delta T} \Delta T_{i,\ell} + M_{i,\ell}]}. \tag{8}$$

Multiplying π_{ij} by the total population stock s_i in location i, we derive an expression for the total number of migrants m_{ij} between locations i and j:

$$m_{ij} = \frac{\exp[\beta_I \ln I_j - \beta_H \ln r_j - \beta_{\Delta T} \Delta T_{ij} - M_{ij}]}{\sum_{\ell \in J} \exp[\beta_I \ln I_\ell - \beta_H \ln r_\ell - \beta_{\Delta T} \Delta T_{i\ell} - \beta_M M_{i\ell}]} \times s_i. \tag{9}$$

Because the denominator is a scalar, this is structurally equivalent to an estimable gravity model of migration flows:[4]

$$m_{ij} = \exp\left[\beta_I \ln I_j - \beta_H \ln r_j + \beta_{\Delta T} \Delta T_{ij} + \beta_X X_j + \beta_M \tilde{M}_{ij} + \lambda_i\right] + \varepsilon_{ij}, \tag{10}$$

in which X_j represents additional destination-specific controls and $\tilde{M}_{ij}$ represents an observable proxy of M_{ij}, the utility costs of migration between i and j. In this expression, the origin fixed effect λ_i captures both the size of the origin population s_i and the denominator of Equation (9):

$$\lambda_i = \ln s_i - \ln\left(\sum_\ell \exp\left[\beta_I \ln I_\ell - \beta_H \ln r_\ell - \beta_{\Delta T} \Delta T_{i\ell} + \beta_X X_\ell - \beta_M \tilde{M}_{i\ell}\right]\right). \tag{11}$$

In our panel data setting, we estimate the following extension of Equation (10) to a conditional (fixed effects) model using Poisson pseudo-maximum likelihood (PPML) (Cameron and Trivedi 2013; Wooldridge 2002):

[4] Our main analysis uses a Poisson pseudo-maximum likelihood approach given the large mass of zero bilateral migration flows. However, Appendix Section F shows that this same structure can also be used to derive an estimating equation using OLS. Robustness to OLS estimation is reported in Appendix Table G2.

$$m_{ijt} = \exp\left[\beta_I \ln I_{jt} - \beta_H \ln r_{jt} + \beta_{\Delta T} \Delta T_{ij} + \beta_X X_{jt} + \beta_M \tilde{M}_{ij} + \lambda_{it} + \mu_j\right] + \varepsilon_{ijt}, \tag{12}$$

where origin-year fixed effects λ_{it} absorb all time-varying origin-specific migration push factors, including local income shocks, housing costs, and demographic or policy changes, and destination fixed effects μ_j absorb all time-invariant destination attributes, including amenities, climate and income levels, and other unobserved location fundamentals. We use two measures of migration costs $\tilde{M}_{ij}$—geographic distance (in km) and travel distance (in km) between the population-weighted centroids of each location—as well as the absolute value of the difference in coastal proximity between the two locations. We control for a comprehensive set of destination-level time-varying covariates X_{jt} including the average age of residents and the shares of individuals falling into the following categories: gender, education (complete college education or no college education), marital and parenthood status, occupation (agricultural versus non-agricultural workers), ethnicity (white, black, or hispanic), and economic status (home ownership).

The identifying variation in Equation (12) used to estimate $\beta_{\Delta T}$ is cross-sectional: we compare how migration flows into the same destination j differ across origins i that have distinct temperature distances ΔT_{ij}, conditional on the distance between i and j. In contrast, the identifying variation for β_I, the denominator in our willingness-to-pay expression in Equation (5), is temporal: destination fixed effects absorb average income levels, such that we compare how migration flows from all origins i into destination j change when incomes rise or fall in j over time. We additionally estimate a stacked cross sectional version of Equation (12), in which only origin-year fixed effects are included and all identifying variation is cross-sectional.

3.3 Instrumenting income

Migrants' income may be endogenous to the many unobserved factors that both affect their earnings and influence migratory decisions, such as local economic opportunities or amenities.[5] To address endogeneity concerns, we adapt two traditional instrumental variables to our setting, which rely respectively on plausible exogenous variation in regional industry-

[5] We note that temperature distance ΔT_{ij} is also plausibly endogenous, as it may spatially correlate with other determinants of migratory flows. We refer readers to the many robustness and sensitivity analyses undertaken in Obolensky et al. (2024), which provide evidence to support a causal interpretation and which we replicate in our data and setting in Section 4.

specific employment from Bartik 1991 (Section 3.3.1) and in Chinese exports to high-income countries from Autor et al. 2013 (Section 3.3.2).

Since our dependent variable is measured as the count of migrants, to account for the endogeneity of income, we generalize the standard conditional Poisson model into an instrumental variables setting. To do this, we adopt a control-function approach to the conditional Poisson model (Wooldridge 2002), whereby we include the residual from the first-stage regression in our regression equation of interest, Equation (12).[6]

3.3.1 Bartik instrument

We construct a Bartik-style (shift-share) instrument z_{jt} that is location-year specific and exploits the differential industrial composition of employment in each location in 1990 and industry-specific employment levels. Specifically, our instrument is constructed as:

$$z_{jt} = \sum_{k} \omega_{jk} g_{jkt}, \tag{13}$$

where ω_{jk} is the 1990 share of PUMA j's employment in industry k,[7] and g_{jkt} is the leave-one-division-out employment level in industry k in PUMA j in year t.[8] For each region ℓ, we compute employment in industry k, $g_{\ell kt}$, then we compute the leave-one-region-out employment level for PUMA j in region r, such that

$$g_{jkt} = \frac{1}{8} \sum_{\ell \neq r} g_{\ell kt} \tag{14}$$

3.3.2 China shock

For robustness, we also construct the growth of Chinese import competition as an instrument. To do so, we follow Section 3.3.1 by combining location-specific baseline industry shares

[6] While including the first-stage error purges the estimates of the various selection and endogeneity biases, the standard errors also need to be corrected for the variation coming from the first stage estimation. In future versions of the paper, we will account for the first-stage sampling error in the residuals, and bootstrap the regression using a block-bootstrap procedure where we randomly draw the entire history of a destination with replacement.

[7] Where $\sum_k \omega_{jk} = 1$, $\forall\ j$. To maintain a balanced sample of industries over time, we retain the 2-digit industry codes. There are 89 industries in total.

[8] There are nine regions in the U.S.: New England, Middle Atlantic, East North Central, West North Central, South Atlantic, East South Central, West South Central, Mountain, Pacific. For a list of the states in each division, see here.

with a measure of Chinese exports to high-income countries ("China shock") to construct an exposure measure at the `MIGPUMA` level. Intuitively, locations that were more specialized in industries experiencing larger increases in Chinese import competition are predicted to face larger local labor-demand shocks (Autor et al. 2013). Additional details about the instrument construction are provided in Appendix D.

4 Results

4.1 Baseline

We report our baseline results from the PPML estimation of Equation (12) in Table 1. We find a strong negative association between climate distance both in temperature and precipitation and migration flows across all specifications. In our most conservative specification that accounts for geographic and coastal distance as measures of bilateral migration costs and socio-demographic covariates (column 3), we find that a 1°C increase in temperature distance between origin and destination reduces expected migration flows by approximately 5.7%. As expected, income is a strong pull factor in migration decisions: a 10% increase in destination income is associated with an increase in expected migration flows of about 4.7% (similar in magnitude to the comparable estimate of 3.1% from Kennan and Walker (2011)).

Results are robust to many alternative specifications and sensitivity analyses, including: a stacked cross-sectional specification (Appendix Table G1); a leave-one-state out exercise (Figure G1),[9]; an alternative OLS approach (Appendix Table G2); a specification that estimates semi-elasticities to measures of distance (Appendix Table G3); alternative measures of climate distance (Appendix Table G4); and alternative measures of income (Appendix Table G5).

To address concerns about pre-existing migration networks confounding the effect of climate distance, we augment the baseline specification with controls for historical bilateral migration flows, which proxy for persistent network ties and path dependence. While such controls may be viewed as "bad controls" if networks are themselves an outcome of earlier climate-driven sorting, the estimated effect of climate distance remains stable. Results are robust to conditioning on both historical migration networks in 1850–1940 and more recent bilateral flows from prior census waves (Appendix Table G6). To address spatial correlation

[9] We note that Figure G1 shows that two states—California and Florida—change the magnitude of the temperature distance coefficient substantially. We are currently investigating this further.

in climate, we show sensitivity to increasing our 80-km threshold to define migratory flows and excluding within-state moves (Appendix Table G7). Perhaps intuitively, the negative effect of temperature distance on migrant flows declines in samples restricted to long-distance moves.

These regression results imply large willingness-to-pay estimates, as shown at the bottom of Table 1. In our baseline specification, we estimate that household heads are willing to pay ∼$4,700 in annual income to reduce temperature change by 1°C. This amounts to over 11% of annual income for household heads in our sample, representing a large cost of adjusting to a new long-run climate regime. As expected, this value varies across some of our robustness analyses, falling to ∼$2,700 per 1°C in an OLS specification and rising to ∼$6,700 per 1°C when using summer temperatures only to define temperature distance.

4.2 Directionality in temperature distance

The negative effects of temperature distance on migration flows shown in the previous subsection indicate a revealed preference for maintaining a stable long-run climate. However, this specification is restrictive, as it implicitly assumes homogeneity in response across different baseline climates and across migrants moving to hotter and to colder localities. However, it is possible that the disutility of climate change differs for migrants starting in hot versus cold climates and for migrants moving to hotter versus to colder destinations. This potential heterogeneity is particularly important when considering the implications of these results for long-run climate change, as all origins will be hotter and experiencing continually rising temperatures in the future as anthropogenic climate change unfolds. Here, we estimate more flexible models that relax both sets of assumptions on response homogeneity.

Appendix Table G8 shows that the effect of temperature distance on migration flows is consistently negative across all origin climates. However, the marginal effect of temperature distance is substantially larger for migrants originating in the coldest tercile of PUMAs ($\hat{\beta}_{\Delta T} = -0.37$, $p < .01$) than for those originating from the hottest tercile ($\hat{\beta}_{\Delta T} = -0.08$, $p < .01$). This pattern suggests that residents of cold climates face steeper adjustment costs when moving away from their climatological equilibrium, whether toward warmer or colder destinations. However, they also imply that even in a future in which all origins are substantially hotter than they are today due to climate change, additional changes in the climate are costly.

A future under climate change implies additional warming for all localities. Thus, to apply these estimates to the valuation of anthropogenic climate change, it is critical to assess how

Table 1: PPML: Weighted bilateral flows 2000-2016.

Dependent Variable:	Migration count		
Model:	(1)	(2)	(3)
Variables			
Temperature distance	-0.1372***	-0.0569***	-0.0568***
	(0.0020)	(0.0015)	(0.0015)
Precipitation distance	-0.0258***	-0.0047***	-0.0047***
	(0.0003)	(0.0003)	(0.0003)
Income (adj. housing costs)	0.3413***	0.3897***	0.4744***
	(0.0644)	(0.0640)	(0.0641)
Coastal distance (in km)		-0.0016***	-0.0016***
		(2.92×10^{-5})	(2.92×10^{-5})
Geographic distance (in km)		-0.0009***	-0.0009***
		(9.29×10^{-6})	(9.29×10^{-6})
Age			-0.0741***
			(0.0075)
Male			-0.1675
			(0.2291)
Married			0.5790*
			(0.3220)
Children			-0.3146***
			(0.1209)
Farm			-1.361
			(1.072)
Black			0.0318
			(0.3389)
Hispanic			0.4161
			(0.3547)
Homeowner			-1.314***
			(0.2892)
College (compl.)			0.1383
			(0.3078)
Fixed-effects			
Year-Origin	Yes	Yes	Yes
Destination	Yes	Yes	Yes
Fit statistics			
WTP 1C	15,916.6	5,777.7	4,742.2
Temperature Distance (mean)	3.8	3.8	3.8
Income (mean)	39,594.6	39,594.6	39,594.6
Migration count (mean)	7.855	7.855	7.855
Observations	4,017,570	4,017,570	4,017,570

Clustered (Origin-Destination) standard-errors in parentheses
*Signif. Codes: ***: 0.01, **: 0.05, *: 0.1*

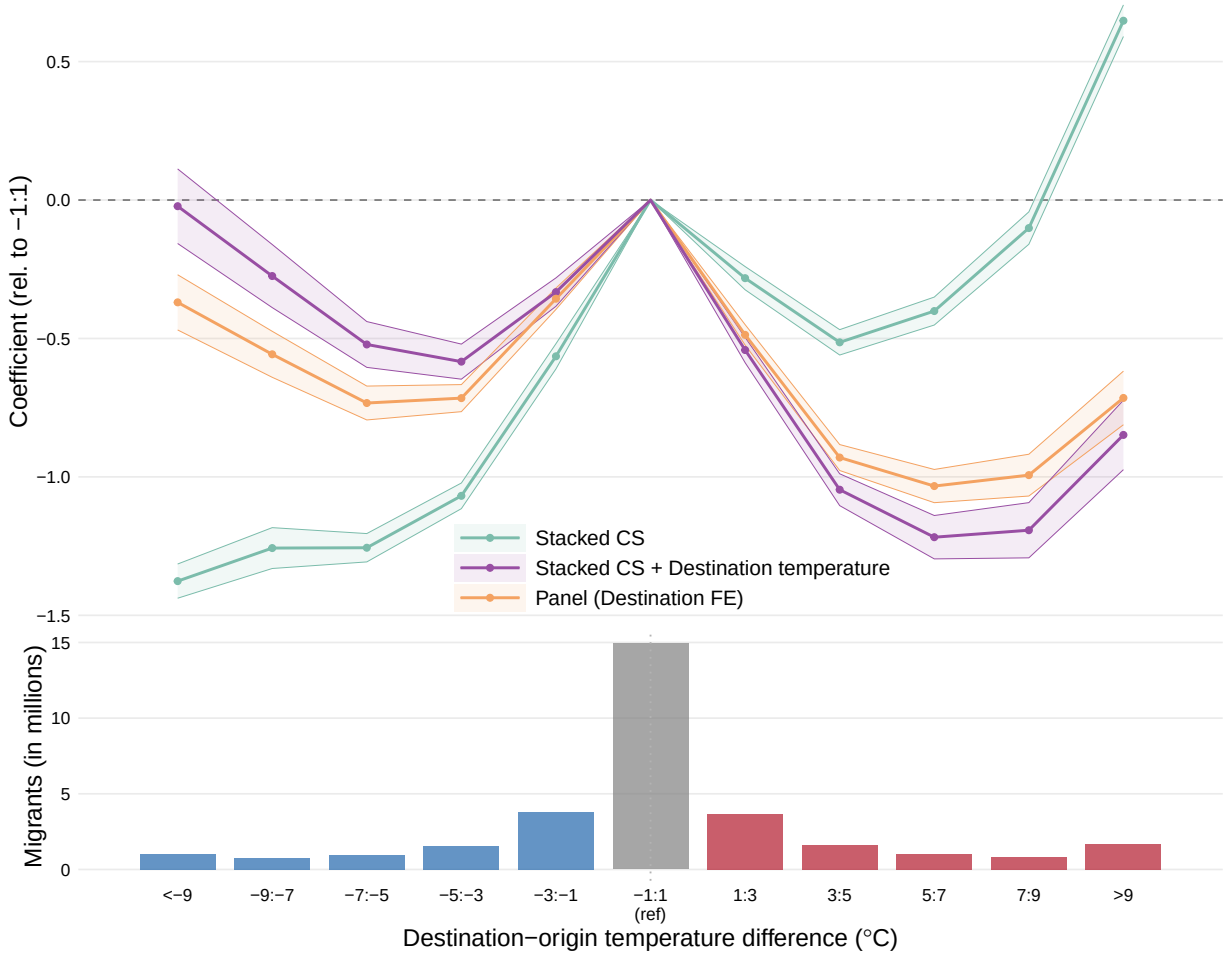
migratory responses depend on climate differences that are positive (indicating a warmer climate than the origin) versus those that are negative (indicating a cooler climate than

the origin). To examine such directional asymmetries, in Appendix Table G9 we further split the sample not only by origin climate, but also by whether the move is toward a warmer or colder destination. In a cross-sectional specification (noting that destination fixed effects are collinear with temperature distance in this specification, making the panel model inestimable), we find that migrants from hot origins penalize moves to warmer destinations (Panel A, column 6), while those from cold and mild origins are attracted to them (Panel A, columns 2 and 4). This finding is consistent with the well-documented Sunbelt migration pull documented in Figure A1. However, once we exclude the three largest Sunbelt destination states (Arizona, Florida, and Texas), this directional asymmetry collapses: temperature distance uniformly discourages migration regardless of origin climate or direction of the move, reinforcing that the Sunbelt premium reflects destination-specific economic and amenity attributes rather than an intrinsic preference for warmth (Panel B).

Figure 3 provides nonparametric evidence from signed temperature bins that reinforces this conclusion. Here, we estimate a panel regression in which the linearity of the temperature distance variable is replaced by a set of binned binary variables indicating whether a migration flow from i to j falls into one of 11 bins of temperature change, ranging from > 9°C cooler to > 9°C warmer. In the panel specification shown in orange, where destination fixed effects control for average climatic and economic conditions, both warm and cold moves reduce migratory flows relative to small temperature changes, with the penalty escalating monotonically in temperature distance.

In contrast, the cross-section without destination controls is shown in green and shows that migration flows *increase* with large temperature increases (>9°C). While this finding is consistent with panel A from Appendix Table G9, this finding reverses entirely once destination temperature is controlled for. This decomposition clarifies the role of our panel design: origin-by-period and destination fixed effects control for all characteristics of both locations, isolating the bilateral climate friction between origin-destination pairs. The estimating variation compares flows to the *same* destination from different origins: among all origins sending migrants to Houston, those from climatically similar locations send more than those from climatically distant locations, conditional on income and other controls. The Sunbelt pull—and all other destination-specific amenities—is absorbed; what remains is the cost of deviating from one's climatic equilibrium.

Figure 3: Nonlinear and asymmetric migration response to destination-origin temperature differences



Notes: Each coefficient corresponds to a bin of the destination mean temperature minus the origin mean temperatre, relative to the omitted category (-1°C to 1°C). Estimates are from a PPML regression model of bilateral migration flows between PUMA pairs. The "Stacked CS" specification includes origin-year fixed effects; the "Stacked CS + Destination Temperature" additionally controls for destination mean temperature and precipitation levels; and the "Panel" model adds destination fixed effects. All specifications include precipitation distance, log housing-cost-adjusted income, geographic distance, and demographic controls. Shaded bands represent 95% confidence intervals with standard errors are clustered at the origin-destination pair level. The bottom panel shows the distribution of migrants across temperature difference bins (in millions).

4.3 Heterogeneity by sociodemographics

Here we estimate fold-specific responses of migration flows to temperature distance and fold-specific income estimated in a PPML panel between 2000 and 2016 for a set of sociodemographic groups. The dependent variable is the number of migrants per origin–destination–year–fold

(e.g., the number of people under age 65 moving from Los Angeles to Chicago in 2011). Tabular results are shown in Table G10 and Figure G10 displays results graphically.

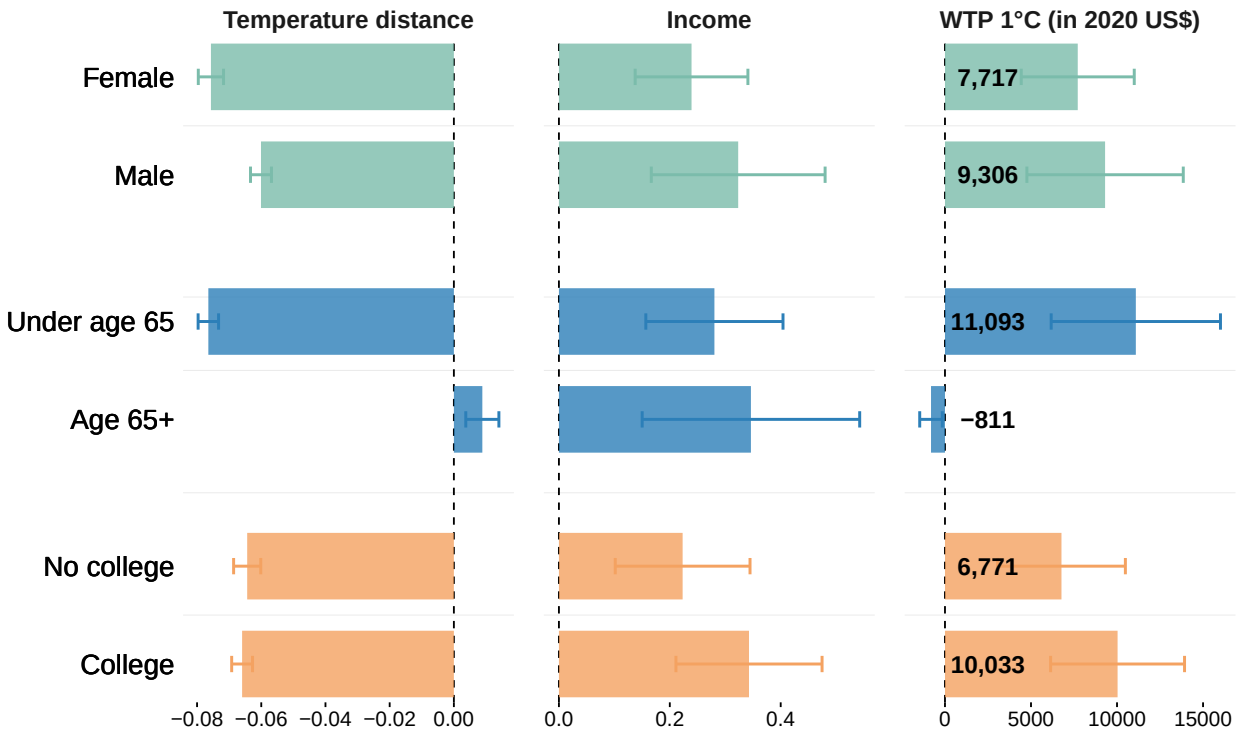
Across nearly all specifications, temperature distance has a negative and precisely estimated coefficient, indicating that migrants is most reference category groups (women, people over aged 65, and people with a college education) are significantly less likely to move to destinations whose climate differs more from their origin. The exception is age; we find that migrants over the age of 65 have a very small *positive* coefficient on temperature distance, while a 1°C increase in temperature distance reduces bilateral migration flows by roughly 6–8% for women and those with a college degree.

In Column (1), the interaction between temperature distance and male is positive, partially offsetting the baseline negative effect. We find that male migrants are ∼20% less sensitive to climate dissimilarity than female migrants. In Column (2), younger migrants (under age 65) exhibit substantially higher sensitivity to temperature distance relative to older migrants, as reflected in the large and negative interaction term. Column (3) shows some heterogeneity by education: migrants without a college degree are slightly less climate-sensitive, but this effect is statistically insignificant. To account for difference in the climate-income tradeoff across different demographic groups, we also allow the migration income elasticity to vary by folds. While we find a strong positive and significant income elasticity across all folds, we do not uncover statistically significant heterogeneity across folds.

Given the large differences uncovered in temperature distance sensitivity by age, in Figure 5 we explore age heterogeneity in more detail, showing results for 8 different bins of ages of the head of household. Results are strikingly distinct across ages; the top panel shows that temperature distance has a 15 times larger effect on migratory flows for the youngest heads of household (ages 15-25) than it does for the oldest (ages >85). Effects approach zero nearly monotonically, crossing zero at the retirement ages of 65-75. In contrast, income elasticities shown in the middle panel rise with age until retirement, falling to small and statistically insignificant by the 75-85 year old age category.

The implied willingness-to-pay (WTP) measures reported at the bottom of Table G10 and Figure 5 translate these estimates into economically meaningful magnitudes. The right column in Figure 4 displays these results graphically. Across nearly all folds, the WTP to avoid a 1°C change long-run average temperature is sizable and varies with demographic characteristics. While average willingness to pay across the entire sample is ∼$4,742 per 1°C (column 3, Table 1), the value is slightly negative for people over the age of 65 (column 2, Table G10), consistent with retirement migration to climatically different destinations. WTP

Figure 4: Willingness to pay for changes in climate by demographic groups

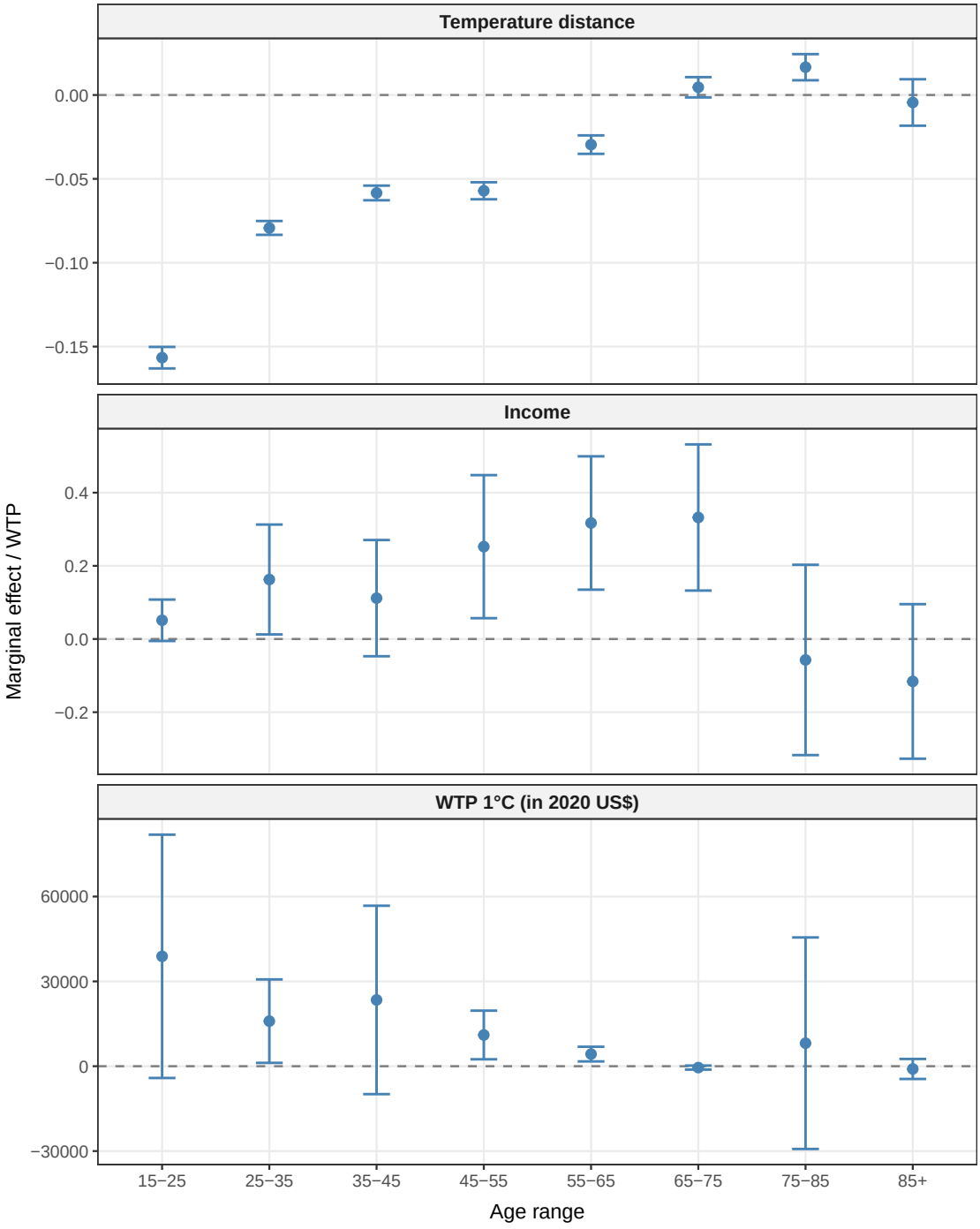


Notes: Each panel displays estimates from three separate PPML regressions, each interacting the key regressors with a binary demographic indicator. The left panel shows the semi-elasticity of migration with respect to temperature distance between origin and destination. The middle panel reports the elasticity of migration with respect to log destination income adjusted for housing costs. The right panel shows the implied willingness to pay (WTP) to avoid a 1°C increase in temperature distance, in 2020 US$, computed as the negative ratio of the temperature semi-elasticity to the income elasticity scaled by group-specific weighted average adjusted household income. Confidence intervals are constructed via the delta method using the cluster-robust variance-covariance matrix, with standard errors clustered at the origin-destination pair level. All models include origin-year-group and destination-group fixed effects. Tabular results reported in Table G10.

per 1°C is ∼$10,000 for household heads with a college degree and ∼$6,800 for those without. WTP is strikingly similar for women and men.[10] While we are still unpacking the possible mechanisms behind these results, they are roughly consistent with results from Obolensky et al. (2024) suggesting that migrants build climate-specific human capital, particularly in climate-sensitive jobs. To the extent that this human capital is most relevant in the working age population and in jobs that may require less education (e.g., farming, construction), our heterogeneity in WTP aligns with this intuition.

[10] We note that while women and men respond differentially to temperature distance in terms of their migration behavior, they also respond differently to income, leading to very similar estimated WTP.

Figure 5: Willingness to pay for changes in climate by ten-year age group



Notes: The top panel shows the semi-elasticity of migration with respect to temperature distance. The middle panel reports the elasticity of migration flows with respect to log income at the destination, adjusted for housing costs. The bottom panel shows the implied willingness to pay (WTP) to avoid a 1°C increase in temperature distance, in 2020 US$, computed as the negative ratio of the temperature semi-elasticity to the income elasticity, scaled by the weighted average adjusted household income of each age group. Confidence intervals are constructed via the delta method using the cluster-robust variance-covariance matrix, with standard errors clustered at the origin-destination pair level. All estimates are drawn from a single model that pools across age groups and recovers age-specific effects through interactions.

4.4 Instrumenting income

Table 2 reports instrumental variables estimates that address potential endogeneity of destination income in Equation (12). Because the baseline specification is estimated by PPML, we implement this IV using a control-function approach (Wooldridge 2002). The table presents, for comparison, the baseline PPML estimates (column 1), the first-stage income equation estimated by OLS (columns 2 for the shift-share instrument and column 4 for the China shock instrument), and the second-stage IV-PPML estimates including the first-stage residuals (column 3 for the shift-share instrument and column 5 for the China shock instrument).

The first-stage regression relates log destination income (adjusted for housing costs) to a shift-share industry employment growth instrument or China shock instrument (see Section 3.3), controlling for the same set of fixed effects and covariates used in the baseline specification. Both instruments are strongly predictive of income, with precisely estimated coefficients and F-statistics far above conventional thresholds for weak instruments.

Columns (3) and (5) report the second-stage IV-PPML estimates. The coefficients on income are nearly unchanged relative to the baseline (0.48 vs. 0.47), and the estimated effects of temperature and precipitation distance are also stable. The implied WTP is \$4,653 per 1°C, very similar to the baseline estimate. The insensitivity of the income coefficient to instrumentation suggests that endogeneity of destination income is not a first-order concern in our setting. In what follows, we use the baseline PPML coefficients from column (1) to compute a hedonic estimate of U.S. Social Cost of Carbon.

Table 2: IV-PPML regressions using Bartik employment and China shock as instruments.

Dependent Variables:	Migration Count	log(Income adj.)	Migration Count	log(Income adj.)	Migration Count
	(1)	(2)	(3)	(4)	(5)
Estimation method:	PPML	OLS (1st stage)	IV-PPML (2nd)	OLS (1st stage)	IV-PPML (2nd)
Variables					
Temperature distance	-0.0568***	6.26×10^{-21}	-0.0568***	7.28×10^{-21}	-0.0568***
	(0.0015)	(7.77×10^{-17})	(0.0015)	(7.77×10^{-17})	(0.0015)
Income (adj. housing costs)	0.4744***		0.4830***		0.4830***
	(0.0641)		(0.0642)		(0.0642)
Shift-share industry employment		0.0272***			
		(0.0014)			
China shock				-0.0098***	
				(6.94×10^{-5})	
Residuals first stage			-0.0414		-0.0447
			(0.0720)		(0.0723)
Origin-Year FE	Yes	Yes	Yes	Yes	Yes
Destination FE	Yes	Yes	Yes	Yes	Yes
Socio-demographic controls	Yes	Yes	Yes	Yes	Yes
F-stat		358.9		20,096.5	
p-value		2.2e-16		2.2e-16	
WTP 1C	4,742.2		4,652.8		4,652.8
Temperature Distance (mean)	3.8	3.8	3.8	3.8	3.8
Income (mean)	39,594.6		39,594.6		39,594.6
Migration count (mean)	7.9		7.9		7.9
Observations	4,017,570	4,018,578	3,988,770	4,018,578	3,988,770

Shift-share industry employment is in millions of workers. China shock is in millions of 2020 US$. *Signif. Codes: ***: 0.01, **: 0.05, *: 0.1*

5 Estimating a hedonic social cost of carbon

Here we translate revealed preference estimates of the value of climate change into estimates of the total damages incurred across the United States by each marginal ton of CO_2 emissions. That is, we compute a hedonic social cost of carbon (SCC) for the United States population.

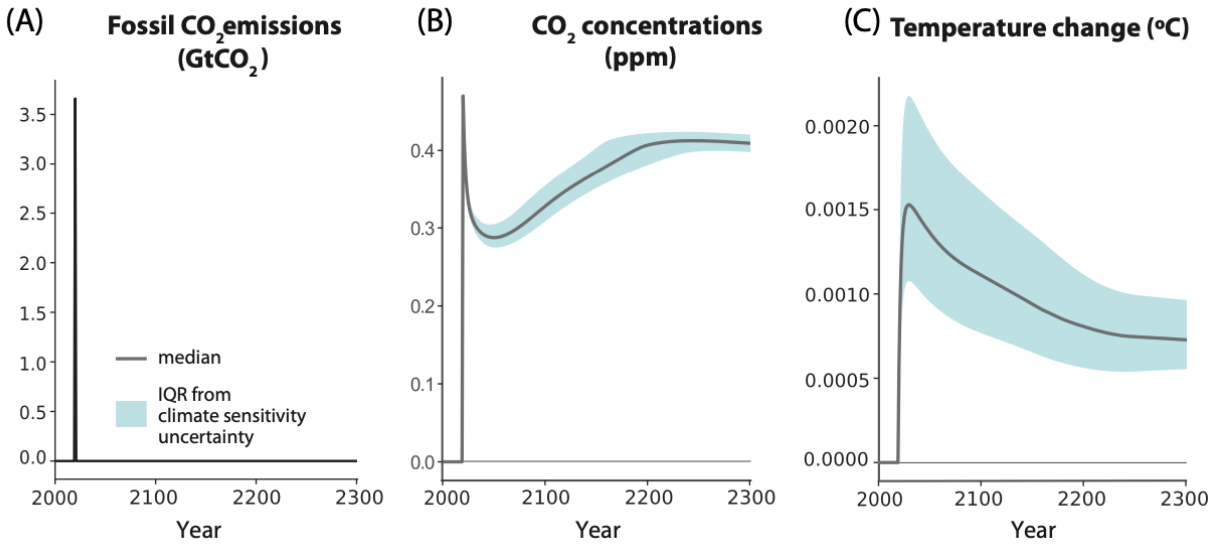
Figure 6 demonstrates the dynamic effect of a present-day pulse of CO_2 on the long-run global climate, as estimated using the FAIR simple climate model.[11] Panel A illustrates a large pulse[12] of CO_2 injected into the atmosphere, on top of a baseline trajectory of warming. Panel B shows that this pulse of CO_2 has a nonlinear near-term effect on cumulative CO_2 concentrations in the atmosphere, as ocean uptake is initially strong but decays with time.

[11] This is a state-of-the-art probabilistic global climate model used by the U.S. Environmental Protection Agency among many others to compute SCC estimates.

[12] Following Climate Impact Lab (2022), we use a pulse of $3.66GtCO_2$ because the climate model cannot resolve impacts of smaller quantities of CO_2. We then rescale resulting effects on global mean surface temperature to recover impacts per ton of CO_2.

Panel C shows the nonlinear and enduring effect of this single pulse of CO_2 on global mean surface temperature (GMST), demonstrating that temperature is elevated even 300 years after a change in emissions. The SCC calculation computes the marginal damages in each year caused by this change in temperature, and discounts the sum to present value.

Figure 6: Change in emissions and temperature due to a marginal emissions pulse



Note: Based on the FAIR simple climate model. Figure replicated from Carleton et al. (2022).

Formally, the SCC in year t is defined as the present discounted value of all damages caused by emission of one metric ton of CO_2 in t:

$$SCC_t = \int_{s=t}^{\infty} e^{-\delta(s-t)} \frac{dU_s}{dT} \frac{dT_s}{dE_t} ds, \tag{15}$$

where t is the "pulse year", $\frac{dU_s}{dT}$ is the marginal WTP for an increase in temperature, $\frac{dT_s}{dE_t}$ is the impact of emissions in year t on global mean surface temperature T in year s, and δ is the discount rate (in what follows, we set the discount rate to δ=2% for consistency with current SCC papers estimating US SCC values). Here, we integrate WTP over all American households, making this a United States SCC, as opposed to the more standard global calculation (Carleton and Greenstone 2022).

We compute a discrete approximation to Equation 15 using our WTP estimates from Section 4. Importantly, this calculation accounts for future adaptation by assuming individuals born in the future are adapted to their birth year climate. Specifically, we estimate the SCC as:[13]

[13] Like other work (e.g., Rennert, Errickson, et al. (2022)), we stop integration at 2300 given lack of projection data on climate and socioeconomics after this date.

$$SCC_t = \begin{cases} \sum_{s=t}^{2300} e^{-\delta(s-t)} \frac{-\hat{\beta}_{\Delta T}}{\hat{\beta}_I} \overline{I}_s \sum_{a=1}^{21} pop_{a,s} \frac{dT_s}{dE_t} & \text{if } a \geq s-t \\ \sum_{s=t}^{2300} e^{-\delta(s-t)} \frac{-\hat{\beta}_{\Delta T}}{\hat{\beta}_I} \overline{I}_s \sum_{a=1}^{21} pop_{a,s} \left(\frac{dT_s}{dE_t} - \frac{dT_{s-a}}{dE_t} \right) & \text{if } a < s-t, \end{cases} \tag{16}$$

where a indicates one of 21 age groups included in the UN Population projections and $\frac{dT_{s-a}}{dE_t}$ indicates the warming in the year $s-a$ caused by emissions in year t, where a indicates the midpoint of each of the 21 age groups. This age adjustment computes the hedonic SCC only relative to each individuals' birth year. That is, for people born into the United States in year 2070, we assume they value climate distance relative to the predominant climate of their birth year and location only.

In this calculation, we replace the WTP term $\frac{dU_s}{dT}$ with our estimated WTP $-\frac{\hat{\beta}_{\Delta T}}{\hat{\beta}_I}\overline{I}_s$ and scale the estimate from an individual household head to the U.S. population using pop_s, a projected population value (described below). To operationalize Equation (**??**), we construct annual estimates of willingness to pay, population, and temperature responses to a marginal CO_2 pulse, and aggregate discounted damages over the horizon 2030-2300 (we use a pulse year of 2030 for comparability to recent papers estimating U.S. SCC values for this year, as shown below).

To construct time-varying estimates of the monetized value of damages, we map our micro-founded estimates of marginal willingness to pay per degree of warming into economy-wide dollar values. Our empirical estimates are expressed in Census units (household sample weights and household income). To scale these to observed aggregates, we compute conversion factors using historical U.S. population and GDP data from the World Bank World Development Indicators.[14] These scalars are then used to rescale projected population and income paths from the Data-driven Spatial Climate Impact Model (DSCIM) socioeconomic module (Climate Impact Lab 2022),[15] yielding annual population levels and GDP per capita consistent with national aggregates.

To estimate how the global climate responds to emissions (i.e., $\frac{dT_s}{dE_t}$ in Equation **??**), we obtain the climate response to a marginal emissions pulse from the FAIR model (Millar et al. (2017), as implemented within the DSCIM climate module). We use model-simulated global mean surface temperature time paths under a one-time CO_2 pulse in 2030 and subtract the corresponding control trajectory to recover $\frac{dT_s}{dE_{2030}}$ for each future year s. We adjust the change in global mean surface temperature by a scalar to reflect the faster rate of warming

[14] Specifically, we estimate a scalar mapping between Census household weights and total U.S. population, and between ACS household income and observed GDP per capita.

[15] Population and income paths from DSCIM come originally from Rennert, Prest, et al. (2022). We access them from DSCIM, here: https://github.com/ClimateImpactLab/dscim-facts-epa/releases/tag/v0.5.0.

in the U.S., as compared with the global mean.

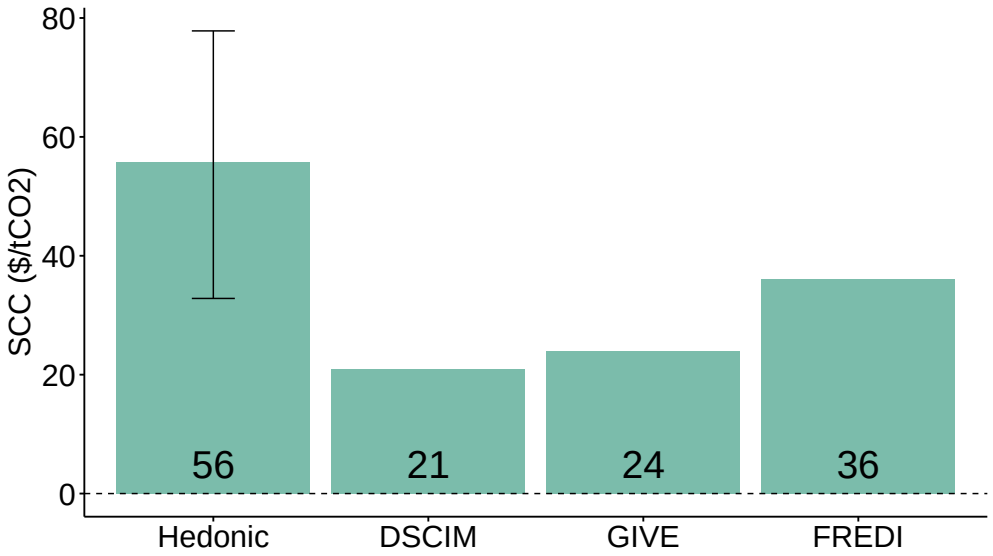
Third, we combine these components to compute annual damages. For each year s, we multiply (i) the median marginal willingness to pay for a 1°C increase, obtained as the ratio $\hat{\beta}_{\Delta T}/\hat{\beta}_I$ times projected income per capita $\overline{I_s}$, (ii) projected household population by age cohort $pop_{a,s}$, (iii) the temperature response to the 2030 emissions pulse $\frac{dT_s}{dE_t}$, and (iv) the appropriate discount factor $e^{-\delta(s-2030)}$. Annual damages are converted from gigatons of CO_2 to metric tons using a factor of 3.66×10^9. We then sum discounted annual damages over 2030–2300 to obtain the SCC in dollars per ton of CO_2.

Finally, we propagate uncertainty from the climate module by computing lower and upper bounds on the SCC using the 2.5th and 97.5th percentiles of the temperature response across a probabilistic set of 10,000 climate model runs, holding socioeconomic variables fixed at their median values. This procedure yields a discrete approximation to Equation (15) that fully accounts for the nonlinear warming paths following a CO_2 pulse. In future versions of the paper, we will additionally propagate statistical uncertainty through the SCC step, accounting for variability not only in the climate response but also in the estimated WTP.

Figure 7 shows our hedonic migration-based estimate of the U.S. social cost of carbon and compares it to the existing enumerative SCC literature (Kopits et al. 2025). Leading U.S.-specific enumerative estimates range from \$21/mtCO_2 in DSCIM (mortality, energy, agriculture, coastal, labor) (Climate Impact Lab 2022), to \$24/mtCO_2 in the Greenhouse Gas Impact Value Estimator (GIVE) (mortality, energy, agriculture, coastal) (Rennert, Errickson, et al. 2022), to \$36/mtCO_2 in EPA's Framework for Evaluating Damages and Impacts (FrEDI) (EPA 2024).

Our estimate of the SCC is \$56/mtCO_2 (2020\$), with a 95% confidence interval accounting for climate uncertainty spanning \$33.9 to \$79.3. Our approach captures welfare losses of adjusting to climate change that are revealed through migration responses, a channel that is complementary to those recovered by existing enumerative models. Specifically, our estimates reflect the amenity and productivity costs of *adjusting* to a new climate. In contrast, while some other models account for the benefits of adaptation, they rarely calibrate the costs of this adjustment. When such costs are estimated (e.g., Carleton et al. (2022) for mortality, a component of DSCIM), they are only loosely calibrated to data and represent costs associated with an individual category of climate damages. In contrast, our revealed preference estimates include all adjustment costs, whether those pertain to nonmarket or market effects of climate change. The fact that our estimate is larger in magnitude than existing models implies a critical role of adaptation costs in the aggregate damages from

Figure 7: U.S. SCC compared to estimates from the existing literature.



Notes: Values shown represent the present discounted value of damages caused by emission of one marginal ton of CO_2 in 2030. The "hedonic" estimate represents the SCC recovered in this paper. See text for details on the other three models.

climate change.

6 Discussion

This paper proposes a novel revealed preference approach to valuing the costs of climate change, using internal U.S. migration as a laboratory in which individuals reveal their willingness to accept climatological change in exchange for real income. Our estimates imply that household heads require approximately $4,742 in additional annual income to tolerate a 1°C departure from their long-run climatic equilibrium. Translating these micro-founded willingness-to-accept values into a U.S. social cost of carbon yields an estimate of $56/mtCO, exceeding existing SCC estimates derived from enumerative models building sector-specific damage estimates and pointing to the importance of adaptation costs and amenity values in aggregate climate damages.

Several features of our approach warrant discussion. First, a natural concern is whether migration-based revealed preferences are externally valid as a guide to the long-run costs of climate change. Migrants are a self-selected population, and the margins of adjustment open to them may not map cleanly onto the experience of a population that adapts in place to

gradual warming. To the extent that non-movers face higher adjustment costs than movers, our estimates would provide a lower bound on aggregate welfare losses. At the same time, migration provides a particularly clean laboratory for climate valuation precisely because it generates large, discrete, and observable shifts in climatological exposure, of a magnitude comparable to projected 21st-century warming. The robustness of our estimates across many specifications and instruments gives us confidence that the core climate-income tradeoff we recover is not an artifact of selection or endogeneity.

Second, our approach captures a dimension of climate costs—the welfare loss of adapting to a new long-run climatic equilibrium—that is largely absent from existing integrated assessment models. Enumerative approaches typically aggregate physical damages across sectors such as mortality, energy demand, agriculture, and coastal flooding, and while some account for the benefits of adaptation, few systematically calibrate the costs of the adjustment process itself. Our revealed preference estimates implicitly aggregate across all channels through which climate change affects individual welfare, including non-market amenity values. The gap between our hedonic SCC of \$56/mtCO_2 and leading enumerative estimates ranging from \$21 to \$36/mtCO_2 is suggestive of the quantitative importance of these omitted margins.

Third, the heterogeneity in willingness to pay across demographic groups is novel, but insufficiently explored in the current draft of the paper. We uncover a striking age gradient we document, with climate sensitivity declining nearly monotonically from young household heads to retirees. In contrast, the relative similarity of WTP across genders and by education point to climate adjustment as a broadly shared burden. In future versions of the paper, we aim to examine the mechanisms behind these differences in more detail.

Our approach has important limitations. Our sample covers heads of household in the continental United States between 2000 and 2016, and it is an open question whether our estimates generalize to other time periods or to populations that are less mobile. The SCC calculation relies on assumptions about how future generations value climate relative to their birth-year baseline, and the propagation of socioeconomic uncertainty into the SCC remains incomplete in the current draft. More broadly, while our estimates capture the costs of adjusting to a new climatic equilibrium, they do not speak to the welfare consequences of climatic volatility or extreme events. Looking ahead, the "migration as a laboratory" framework developed here is, in principle, portable. Applied to migration data in other countries, particularly those with greater internal climate gradients or larger projected warming, it could contribute bottom-up building blocks to a globally aggregated hedonic SCC. It could also be extended to examine other dimensions of climate beyond mean temperature, including precipitation variability, humidity, or the frequency of extreme heat days. We view these

extensions as a promising agenda for future research on the revealed preference valuation of a changing climate.

References

Albouy, David, Walter Graf, Ryan Kellogg, and Hendrik Wolff. 2016. "Climate amenities, climate change, and American quality of life." *Journal of the Association of Environmental and Resource Economists* 3 (1): 205–246.

Anderson, James E, and Eric Van Wincoop. 2003. "Gravity with gravitas: A solution to the border puzzle." *American economic review* 93 (1): 170–192.

Autor, David H, David Dorn, and Gordon H Hanson. 2013. "The China syndrome: Local labor market effects of import competition in the United States." *American economic review* 103 (6): 2121–2168.

Bartik, Timothy J. 1991. "Who benefits from state and local economic development policies?"

Bayer, Patrick, Nathaniel Keohane, and Christopher Timmins. 2009. "Migration and hedonic valuation: The case of air quality." *Journal of Environmental Economics and Management* 58 (1): 1–14.

Borusyak, Kirill, Rafael Dix-Carneiro, and Brian Kovak. 2022. "Understanding Migration Responses to Local Shocks." *SSRN Electronic Journal,* ISSN: 1556-5068. https://doi.org/10.2139/ssrn.4086847. https://www.ssrn.com/abstract=4086847.

Burke, Marshall, Solomon M Hsiang, and Edward Miguel. 2015. "Global non-linear effect of temperature on economic production." *Nature* 527 (7577): 235–239.

Cameron, Adrian Colin, and Pravin K Trivedi. 2013. *Regression analysis of count data.* 53. Cambridge university press.

Carhart, Mark, Bob Litterman, Clayton Munnings, and Olivia Vitali. 2022. "Measuring comprehensive carbon prices of national climate policies." *Climate Policy* 22 (2): 198–207.

Carleton, Tamma, and Michael Greenstone. 2022. "A guide to updating the US Government's social cost of carbon." *Review of Environmental Economics and Policy* 16 (2): 196–218.

Carleton, Tamma, Amir Jina, Michael Delgado, Michael Greenstone, Trevor Houser, Solomon Hsiang, Andrew Hultgren, Robert E Kopp, Kelly E McCusker, Ishan Nath, et al. 2022. "Valuing the global mortality consequences of climate change accounting for adaptation costs and benefits." *The Quarterly Journal of Economics* 137 (4): 2037–2105.

Climate Impact Lab. 2022. *Data-driven Spatial Climate Impact Model User Manual, Version 092022-EPA.* Technical Report. Prepared for U.S. Environmental Protection Agency. Climate Impact Lab, University of Chicago. https://impactlab.org/research/dscim-user-manual-version-092022-epa/.

EPA, US. 2024. "Technical documentation on the Framework for Evaluating Damages and Impacts (FrEDI)."

Freeman, Richard, Wenquan Liang, Ran Song, and Christopher Timmins. 2019. "Willingness to pay for clean air in China." *Journal of Environmental Economics and Management* 94:188–216.

Glaeser, Edward L, and Kristina Tobio. 2008. "The rise of the sunbelt." *Southern Economic Journal* 74 (3): 609–643.

Heutel, Garth, Nolan H Miller, and David Molitor. 2021. "Adaptation and the mortality effects of temperature across US climate regions." *Review of Economics and Statistics* 103 (4): 740–753.

Himmelberg, Charles, Christopher Mayer, and Todd Sinai. 2005. "Assessing high house prices: Bubbles, fundamentals and misperceptions." *Journal of Economic Perspectives* 19 (4): 67–92.

Internal Revenue Service. 2023. *Publication 521: Moving Expenses.* https://www.irs.gov/forms-pubs/about-publication-521. Accessed: 2026-02-02.

Johnson, Janna E, and Morris M Kleiner. 2020. "Is occupational licensing a barrier to interstate migration?" *American Economic Journal: Economic Policy* 12 (3): 347–373.

Kennan, John, and James R Walker. 2011. "The effect of expected income on individual migration decisions." *Econometrica* 79 (1): 211–251.

Klein Goldewijk, Kees, Arthur Beusen, Jonathan Doelman, and Elke Stehfest. 2017. "Anthropogenic land use estimates for the Holocene – HYDE 3.2." *Earth System Science Data* 9 (2): 927–953.

Kopits, Elizabeth, Daniel Kraynak, Bryan Parthum, Lisa Rennels, David Smith, Elizabeth Spink, Joseph Perla, and Nshan Burns. 2025. "Economic Impacts of Climate Change in the United States: Integrating and Harmonizing Evidence from Recent Studies." *arXiv preprint arXiv:2509.00212.*

Lemoine, Derek. 2018. *Estimating the consequences of climate change from variation in weather.* Technical report. National Bureau of Economic Research.

Mathes, Sophie M. 2025. "The Dynamics Of Residential Sorting And Health: Implications Of Climate Change In The United States." *International Economic Review* 66 (2): 711–756.

Mendelsohn, Robert, William D Nordhaus, and Daigee Shaw. 1994. "The impact of global warming on agriculture: a Ricardian analysis." *The American economic review,* 753–771.

Millar, Richard J, Zebedee R Nicholls, Pierre Friedlingstein, and Myles R Allen. 2017. "A modified impulse-response representation of the global near-surface air temperature and atmospheric concentration response to carbon dioxide emissions." *Atmospheric Chemistry and Physics* 17 (11): 7213–7228.

Obolensky, Marguerite, Marco Tabellini, and Charles Taylor. 2024. *Migration, Climate Similarity, and the Consequences of Climate Mismatch.* Technical report 32035. National Bureau of Economic Research. https://doi.org/10.3386/w32035. https://www.nber.org/papers/w32035.

Poterba, James M. 1984. "Tax subsidies to owner-occupied housing: an asset-market approach." *The quarterly journal of economics* 99 (4): 729–752.

Rennert, Kevin, Frank Errickson, Brian C Prest, Lisa Rennels, Richard G Newell, William Pizer, Cora Kingdon, Jordan Wingenroth, Roger Cooke, Bryan Parthum, et al. 2022. "Comprehensive evidence implies a higher social cost of CO2." *Nature* 610 (7933): 687–692.

Rennert, Kevin, Brian C Prest, William A Pizer, Richard G Newell, David Anthoff, Cora Kingdon, Lisa Rennels, Roger Cooke, Adrian E Raftery, Frank Errickson, et al. 2022. "The social cost of carbon: advances in long-term probabilistic projections of population, GDP, emissions, and discount rates." *Brookings Papers on Economic Activity* 2021 (2): 223–305.

Sinha, Paramita, Martha L Caulkins, and Maureen L Cropper. 2018. "Household location decisions and the value of climate amenities." *Journal of Environmental Economics and Management* 92:608–637.

Timmins, Christopher. 2007. "If you cannot take the heat, get out of the cerrado. . . recovering the equilibrium amenity cost of nonmarginal climate change in Brazil." *Journal of Regional Science* 47 (1): 1–25.

Wooldridge, Jeffrey M. 2002. "Econometric analysis of cross section and panel data MIT press." *Cambridge, ma* 108 (2): 245–254.

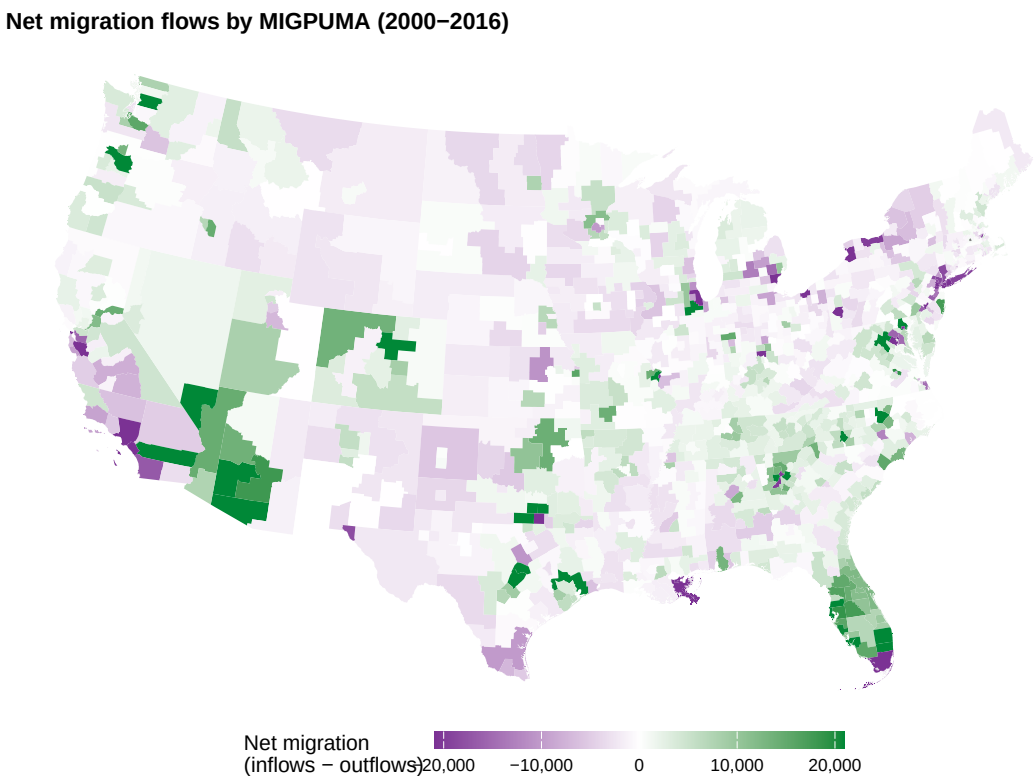
Wrenn, Douglas H. 2024. "The Effect of Natural Disasters and Extreme Weather on Household Location Choice and Economic Welfare." *Journal of the Association of Environmental and Resource Economists* 11 (5): 1101–1134.

Appendix: "A Hedonic Social Cost of Carbon: Evidence from US Migration"

Tamma Carleton, Marco Tabellini, Charles A. Taylor, Guglielmo Zappalà

A Appendix Figures

Figure A1: Net migration flows



B Detailed construction of the bilateral and fold-level data

This appendix describes the construction of the migration PUMA (MIGPUMA) level datasets used in our flow and fold regressions.

B.1 Harmonizing migration PUMAs over time

We take migration PUMAs (MIGPUMAs) as the spatial unit. Because both PUMA and MIGPUMA definitions differ across censuses, we use crosswalks to map all individual records into a harmonized migration geography.

- **National migration PUMA identifiers**: We construct *national* migration PUMA codes as

$$\texttt{NAT_MIGPUMA} = \texttt{STATEFIP}_s \circ \texttt{MIGPUMA}_m$$

  where $\circ$ denotes string concatenation of the 2-digit state FIPS and the 3- or 5-digit MIGPUMA code, padded with leading zeros as needed. This yields a unique national code for each MIGPUMA

- **Year 2000**: The 2000 census uses 2000 PUMAs and three-digit migration PUMAs. We use the 2000 PUMA–to–MIGPUMA crosswalk to map each current PUMA to a three-digit MIGPUMA and then form the national code (state FIPS + 3-digit MIGPUMA). This national MIGPUMA defines the destination j. Origins are constructed from the IPUMS migration variables `MIGPUMA5` and `MIGPLAC5`. We treat codes indicating "abroad", "same house", or "not in universe" as missing, and restrict to domestic states. For valid origin records we again combine previous state and 3-digit MIGPUMA to obtain the origin code i.

- **Years 2006 and 2011**: For 2006 and 2011 ACS cross-sections, PUMAs are still in the 2000 definition, but migration information is stored in `MIGPUMA1`. We map current PUMAs to the 2000 MIGPUMA crosswalk to define destinations j, and we construct origins i from `MIGPUMA1` and `MIGPLAC1`, dropping foreign or non-continental origins. As above, we build national MIGPUMA identifiers by concatenating state FIPS and the three-digit MIGPUMA code.

- **Year 2016**: For the 2016 ACS, the PUMA and MIGPUMA definitions change, so we use the 2010 PUMA–to–MIGPUMA crosswalk. We map current 2010 PUMAs to 2010 MIGPUMAs to define destinations j, and build origins from `MIGPUMA1` and `MIGPLAC1`,

dropping foreign or non-continental origins. In this case we use the full five-digit migration PUMA codes in the national identifier (state FIPS + 5-digit MIGPUMA).

In all years, if the origin MIGPUMA is missing (for instance because the household did not move), we impute the origin as the current destination, setting $i = j$ so that stayers enter the data as zero-distance moves.

B.2 Collapsing individual covariates to MIGPUMA place-level covariates

Let h index individuals, j index destination MIGPUMAs, and t index cross-section years. For each individual we retain the following variables: annual nominal income, annual housing cost, house value, rent, and a set of demographic indicators (age, sex, marital status, children, citizenship, birthplace and ancestry, race, education, farm residence, years since migration, etc.). We use the person weight `PERWT` as the sampling weight in aggregation.

For each cross-section t, we construct resident means at the MIGPUMA level by aggregating over all residents (arrivals and stayers) living in destination j:

$$\bar{X}_{jt} = \frac{\sum_{h:\text{dest}(h)=j} w_h X_{ht}}{\sum_{h:\text{dest}(h)=j} w_h},$$

for each variable X in a pre-specified set that includes income, housing cost, house value, rent, age, education, and other demographics. This produces MIGPUMA-specific "context" variables describing the average income, housing costs, and socio-demographics of residents.

We then merge in climate data defined at the MIGPUMA level. Static climate variables (long-run averages of temperature and precipitation over 1960–2000) are constructed by combining area-weighted and population-weighted climate statistics from gridded data within each MIGPUMA. Five-year window climate variables are computed as average temperature and precipitation over the five-year period preceding each cross-section (e.g. 1996–2000 for the year 2000 sample, 2001–2005 for 2006 sample, etc.), again at the MIGPUMA level. These climate variables are attached to the MIGPUMA context and then duplicated with "$_i$" and "$_j$" suffixes to serve as origin- and destination-specific covariates.

The resulting dataset contains one record per MIGPUMA with resident means of income and housing costs, socio-demographic composition, and both static and moving-average climate conditions. We attach these place-level covariates to each individual observation by matching on origin and destination codes, so each individual-level record carries origin and destination

characteristics (X_i, X_j).

B.3 Origin–destination flow matrices

From the individual-level data we construct standard origin–destination matrices. For each cross-section t, and for each ordered pair of MIGPUMAs (i, j), we compute the weighted count of individuals whose origin is i and destination is j:

$$n_{ijt} = \sum_{h:i(h)=i,j(h)=j} w_h$$

These counts are based on ACS/Census person weights and represent (approximate) numbers of individuals or households moving from i to j over the relevant migration lookback window implied by the microdata.

To ensure a constant choice set across origin–destination pairs, we expand each cross-section to the full Cartesian product of observed origins and destinations. Specifically, for each year t we form the set of origin codes $\mathcal{I}_t$ and destination codes $\mathcal{J}_t$ observed in the microdata, take their cross product $\mathcal{I}_t \times \mathcal{J}_t$, and left-join the observed counts n_{ijt}. All missing cells are assigned $n_{ijt} = 0$. We then merge origin and destination context variables (income and housing costs, socio-demographics, and climate) to each (i, j) cell. The resulting expanded matrices for each sample year form the basis of our baseline regression analysis.

B.4 Fold-specific origin–destination data for heterogeneous regressions

To study heterogeneity in migration responses by demographic group, we construct fold-specific origin–destination–group data. A "fold" c is a mutually exclusive category defined on the individual characteristics (e.g., male vs. female; age < 65 vs. ≥ 65; college vs. no college; ethnicity categories).

For a given cross-section t and fold definition, we:

1. **Assign folds.** For each individual h, we define a categorical variable $\texttt{fold}_h \in \mathcal{C}$ according to the chosen group (e.g. $\mathcal{C} = \{\text{Male}, \text{Female}\}$ for the gender fold). We drop observations with missing fold assignments.

2. **Compute fold-specific flows.** We compute weighted flows by (i, j, c):

$$n_{ijct} = \sum_{h:i(h)=i,\ j(h)=j,\ \texttt{fold}_h=c} w_h$$

3. **Compute fold-specific resident means.** For each destination MIGPUMA j and fold c, we compute weighted means of income, housing costs, and demographic characteristics among residents in that fold:

$$\bar{X}_{jct} = \frac{\sum_{h:j(h)=j,\ \texttt{fold}_h=c} w_h X_{ht}}{\sum_{h:j(h)=j,\ \texttt{fold}_h=c} w_h},$$

for variables X in a pre-specified set that includes income, housing cost, house value, rent, age, education, and other demographic. We store these as destination fold-specific context variables and create an analogous set for origin MIGPUMAs by re-labelling j as i.

4. **Attach geographic and climate context.** We merge in origin and destination geography and climate variables (longitude, latitude, state, and climate measures) which are constant across folds.

5. **Expand to the full $i \times j \times c$ grid.** For each fold definition we form the cross product of observed origins, destinations, and fold levels, $\mathcal{I}_t \times \mathcal{J}_t \times \mathcal{C}$, and left-join the observed (i, j, c) flows and fold-specific contexts. Missing triplets are assigned zero flows and retain the appropriate origin and destination contexts for that fold.

The resulting fold-specific datasets contain, for each year t, the complete set of potential origin–destination moves and demographic cells (i, j, c), with associated counts of movers and context variables for origin, destination, and group c. These are the inputs to our heterogeneous *fold* regressions.

C Construction of the housing user-cost measure

This appendix documents the construction of the user-cost rate UC_{ijt} used to impute owner-occupied housing costs in equation (8). Our approach follows the standard user-cost framework in Poterba (1984) and Himmelberg et al. (2005) and the implementation in Wrenn (2024), with some simplifications tailored to our setting.

Throughout, i indexes households, j denotes states, and t denotes census years. For each owner-occupied unit, we observe self-reported house value H_{ijt} (`VALUEH`), mortgage status (`MORTGAGE`), and an annual property tax code (`PROPTX99`) from IPUMS. We combine these microdata with external series for interest rates, house prices, and tax schedules to construct

$$R_{ijt}^{UC} = H_{ijt}\, UC_{ijt}$$

and then define annual housing cost as $C_{ijt} = R_{ijt}^{UC}$ for homeowners and $C_{ijt} = 12 \times \texttt{RENT}_{ijt}$ for renters.

- **Risk-free rates and mortgage rates**: We obtain the nominal risk-free rate r_t^f from the 10-year Treasury constant-maturity yield (FRED series DGS10). For each census year we download the annual average yield and convert it from percent to an annual decimal rate. We merge these values to the IPUMS microdata by census year t.The borrowing rate r_t^m is the annual average 30-year fixed-rate mortgage (FRED series MORTGAGE30US), again converted from percent to decimal and merged by census year.

- **Property tax rates**: Property tax payments are reported in IPUMS as the categorical variable `PROPTX99`, which records ranges of annual property taxes in dollars. Using the codebook cut points, we map each code to a lower and upper bound and assign a point estimate equal to the midpoint of the bracket (or the lower bound for the open-ended top category). Denote this imputed tax payment by TaxPaid_{ijt}. We then compute a household-level property tax rate as

  $$\omega_{ijt} = \frac{\text{TaxPaid}_{ijt}}{H_{ijt}}.$$

  To smooth idiosyncratic reporting error, we aggregate to the level of consolidated PUMA-by-year and use the median rate within each cell,

  $$\omega_{jt} = \text{median}\{\omega_{ijt} : i \in j, t\}.$$

This ω_{jt} enters the user-cost formula in equation (8).

- **Marginal income tax rates**: We assign federal marginal income tax rates using the Historical U.S. Federal Individual Income Tax Rates and Brackets (1862–2021) from the Tax Foundation. For each year we extract the head-of-household schedule, convert bracket thresholds and statutory rates to decimals, and match each observation's total income (`INCTOT`) to the bracket in which it falls. The resulting rate is denoted τ_{ijt} and is allowed to vary across households and years. We do not model state taxes; instead, τ_{ijt} should be interpreted as a reduced-form federal marginal rate.
- **Depreciation and maintenance**: Consistent with the housing literature, we set the combined depreciation and maintenance rate to a constant $\delta = 0.025$, which lies in the range used by Himmelberg et al. (2005) and Wrenn (2024).
- **Expected capital gains**: To capture expected capital gains on owner-occupied housing, we use the Federal Housing Finance Agency (FHFA) House Price Index at the state level (annual, not seasonally adjusted). For each state j and year t between 1980 and 2020 we compute the annual growth rate of the index,

$$g_{jt} = \frac{\text{HPI}_{jt} - \text{HPI}_{j,t-1}}{\text{HPI}_{j,t-1}}.$$

  We then construct a long-run state-specific appreciation rate as the geometric mean of these growth rates,

$$\text{appr}_j = \exp\left(\frac{1}{N_j}\sum_{t=1980}^{2020} \ln(1 + g_{jt})\right) - 1,$$

  where N_j is the number of years with non-missing HPI for state j. The resulting appr_j is attached to all households in state j and enters the user-cost rate in equation (8) as appr_j.
- **Mortgage indicator and tenure**: We define an indicator for having a mortgage,

$$\mathbb{1}_{\text{mort},ijt} = \begin{cases} 1, & \text{if the IPUMS mortgage variable indicates a current mortgage,} \\ 0, & \text{if the unit is owned free and clear or rented.} \end{cases}$$

  For renters we do not compute a user cost; instead, we set their annual housing cost equal to $12 \times \texttt{RENT}_{ijt}$ as described above.

Combining the components above, the after-tax user-cost rate for homeowner i in state j

and year t is

$$UC_{ijt} = r_t^f + (1 - \tau_{ijt})\,\omega_{jt} + \mathbb{1}_{\text{mort},ijt}\,(1 - \tau_{ijt})\,r_t^m + \delta - \text{appr}_j.$$

We set the risk-premium term often included in user-cost expressions to zero, so any residual local risk premia are absorbed by the appreciation term and the error structure in our empirical model. Multiplying UC_{ijt} by H_{ijt} yields the imputed annual user-cost rent R_{ijt}^{UC} used in the main analysis.

D Construction of China shock

This appendix describes the construction of MIGPUMA-level industry employment shares and the shift-share measure of exposure to changes in Chinese import competition.

Our approach follows the standard procedure in Autor et al. (2013) with some simplifications. We assign each employed individual an industry using the IPUMS `IND1990` clarification. Employment counts are constructed using person weights. For each cross section t, we aggregate weighted employment to obtain E_{jkt}, the total employment in destination `MIGPUMA` j and industry k. We then compute local industry shares

$$s_{jkt} = \frac{E_{jkt}}{\sum_{k'} E_{jk't}},$$

where the denominator is total employment in `MIGPUMA` j in year t. Because migration geographies vary over time, we harmonize all industry shares to the harmonized 2000 `MIGPUMA` geography. Industry codes are not perfectly stable over time. To ensure comparability across years, we construct a balanced set of industries common to all sample years and compute shares within this common set.

Let ΔM_{kt} denote the external industry-level measure of the growth in Chinese import penetration for industry k over a specified period. We construct `MIGPUMA`-level exposure as

$$CS_{jt} = \sum_k s_{jk,0}\,\Delta M_{kt},$$

where $s_{jk,0}$ is a baseline (pre-period) employment share (e.g., from 1990). We use the China import data from Autor et al. (2013) and convert the industry code in their data (`SIC87dd`) into our `IND1990` clarification using the crosswalk from the census government.

For heterogeneity analysis by demographic group c ("folds"), we also compute fold-specific

employment counts E_{jkct} and fold-specific employment shares s_{jkct} using the same methods as above, but restricting employment to individuals in fold c. These fold-specific shares allow us to construct group-specific predicted exposure measures when estimating heterogeneous responses.

E Tax adjustment

This appendix describes the construction of an imputed state income tax rate and after-tax income measure used in the analysis.

We use the National Bureau of Economic Research (NBER) TAXSIM state tax tables, which report state income tax liabilities for a set of standardized taxpayer profiles by state and year. TAXSIM reports tax liabilities for a set of standard income levels {10,000, 25,000, 50,000, 75,000, 100,000, 250,000}. So for each state and tax year, we construct income brackets using adjacent points on these grids:

$$(0, 10{,}000],\ (10{,}000, 25{,}000],\ \ldots,\ (100{,}000, 250{,}000],\ (250{,}000, \infty).$$

For each bracket, we compute an average tax rate at the upper endpoint by dividing the reported tax liability by the corresponding income level. We compute these rates separately for the standardized filing-status categories provided by TAXSIM; in our baseline implementation we use the joint-filer series for all observations to obtain a single state-year schedule.[16]

For each household head h observed in census year t residing in state s, we assign a state tax rate based on the individual's state, tax year, and nominal income. Let y_{hst}^{nom} denote nominal pre-tax income. We then perform a range join on (s, t) and the bracket bounds to assign the tax rate corresponding to the bracket containing y_{hst}^{nom}. Denoting the assigned state tax rate by $\widehat{\tau}_{hst}^{\text{state}}$, we define after-tax nominal income as

$$y_{hst}^{\text{nom,after}} \;=\; y_{hst}^{\text{nom}}\,(1 - \widehat{\tau}_{hst}^{\text{state}}).$$

Later we convert after-tax nominal income to constant dollars using the price deflator.

This procedure produces a comparable measure of state income tax burdens that varies by state, year, and income level. Because it relies on standardized TAXSIM profiles and a discrete income grid, the assigned rate should be interpreted as an imputed average tax rate

[16] Because IPUMS does not provide a consistent filing-status measure across all samples and years, we apply a common schedule to all individuals.

schedule rather than an exact household-specific marginal rate. The approach nonetheless captures the primary cross-state and time-series variation in statutory and effective state income tax burdens relevant for after-tax income comparisons.

F Estimation method

From Equation (8), if we take the ratio of migration flows from i to j divided by the "stayers" in i ($\frac{\pi_{ij}}{\pi_{ii}} = \frac{m_{ij}}{s_i}\frac{s_i}{m_{ii}}$), we obtain a formula for migration rates (Borusyak et al. 2022):

$$\frac{m_{ij}}{m_{ii}} = \frac{\exp[\beta_I \ln I_j + \beta_T T_j - \beta_H \ln r_j - \beta_{\Delta T}\Delta T_{ij} - \beta_M M_{ij}]}{\exp[\beta_I \ln I_i + \beta_T T_i - \beta_H \ln r_i - \beta_{\Delta T}\Delta T_{ii} - \beta_M M_{ii}]} \tag{E.1}$$

By definition $\Delta T_{ii} = M_{ii} = 0$. Taking logs we can write

$$\begin{aligned}\ln\left(\frac{m_{ij}}{m_{ii}}\right) &= \beta_I(\ln I_j - \ln I_i) + \beta_T(T_j - T_i) - \beta_H(\ln r_j - \ln r_i) - \beta_{\Delta T}(\Delta T_{ij} - \Delta T_{ii}) - \beta_M(M_{ij} - M_{ii}) \\ &= \beta_I(\ln I_j - \ln I_i) + \beta_T(T_j - T_i) - \beta_H(\ln r_j - \ln r_i) - \beta_{\Delta T}\Delta T_{ij} - \beta_M M_{ij} \end{aligned} \tag{E.2}$$

We can then estimate Equation (E.2) in a panel or stacked cross section approach using OLS.

G Robustness checks for local income variation

This appendix provides evidence on the spatial and temporal properties of our local income measure, motivated by concerns that the identifying variation in destination income may reflect a one-time shock, or exhibit strong spatial clustering that could confound the interpretation of climate-distance trade-offs.

To assess spatial clustering, we compute changes in housing-cost-adjusted income between 2000 and 2011 for each `MIGPUMA`. Appendix Figure F1 maps both the raw dollar change and the log change at the `MIGPUMA` level. For visualization, the dollar-change color scale is winsorized at the 99th percentile to prevent a small number of extreme changes from dominating the legend. The maps show that income changes are not driven by a single region or a small cluster of `MIGPUMA`s; rather, positive and negative changes appear throughout the continental US. While there is expected broad regional structure (reflecting national and regional business-cycle and housing-market dynamics), the variation we use is not concentrated in one corridor or limited to a handful of large metropolitan areas.

We next examine whether income fluctuations are largely time-specific (common across locations) versus location-specific (persistent differences). Using the pooled `MIGPUMA` panel across years, we estimate:

$$\ln(\widetilde{y}_{jt}) = \alpha_j + \lambda_t + \varepsilon_{jt}, \tag{F.1}$$

$$\ln(\widetilde{y}_{jt}) = \lambda_t + \eta_{jt}. \tag{F.2}$$

Equation (F.1) absorbs permanent differences in income levels across `MIGPUMA`s via α_j and common macroeconomic changes via λ_t. The residual ε_{jt} therefore captures deviations from a `MIGPUMA`'s long-run level in a given year, net of aggregate time shocks. Equation (F.2) removes only year effects, so the residual η_{jt} reflects both persistent cross-sectional heterogeneity and transitory changes.

Appendix Figure F2 plots the distribution of ε_{jt} by year using violin plots with jittered points for all `MIGPUMA`s, and overlays markers for a set of major metropolitan areas. The figure shows that the residual distributions remain centered around zero in each year, and their dispersion is broadly stable, indicating that no single year contains unusually large idiosyncratic deviations once `MIGPUMA` and year effects are netted out. Also, the highlighted metropolitan areas tend to lie well within the overall distribution, suggesting that the identifying variation is not exclusively driven by a few large cities. Appendix Figure F3 repeats the exercise using residuals from the year-only specification in (F.2). As expected, disper-

sion increases because persistent cross-sectional differences remain; nevertheless, the relative position of large cities remains representative of the broader distribution.

Taken together, these diagnostics suggest that the variation in housing-cost-adjusted income used in our empirical design is (i) not purely a one-time, spatially concentrated shock, and (ii) not dominated by a small set of metropolitan outliers. The maps indicate geographically broad changes over time, while the residual plots show stable idiosyncratic dispersion after accounting for location and time fixed effects. These patterns support the interpretation that our estimates are informed by widespread cross-sectional and intertemporal variation in local economic conditions rather than by a single period or narrowly localized cluster.

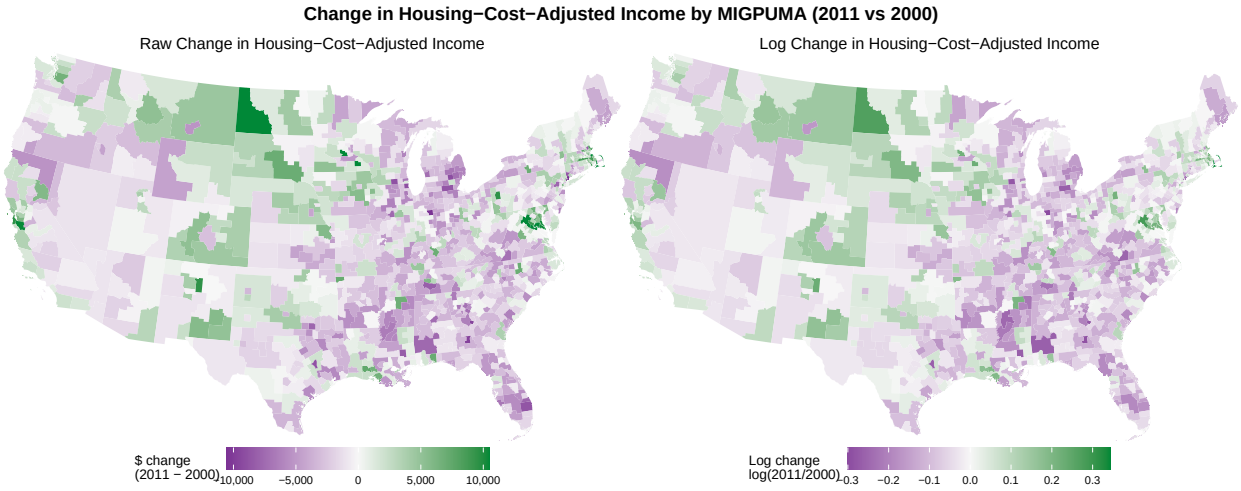


Figure F1: Change in housing-cost-adjusted income by `MIGPUMA`, 2011 vs. 2000. The left panel reports raw dollar changes; the right panel reports log changes. The dollar-change color scale is winsorized at the 99th percentile of absolute changes for readability.

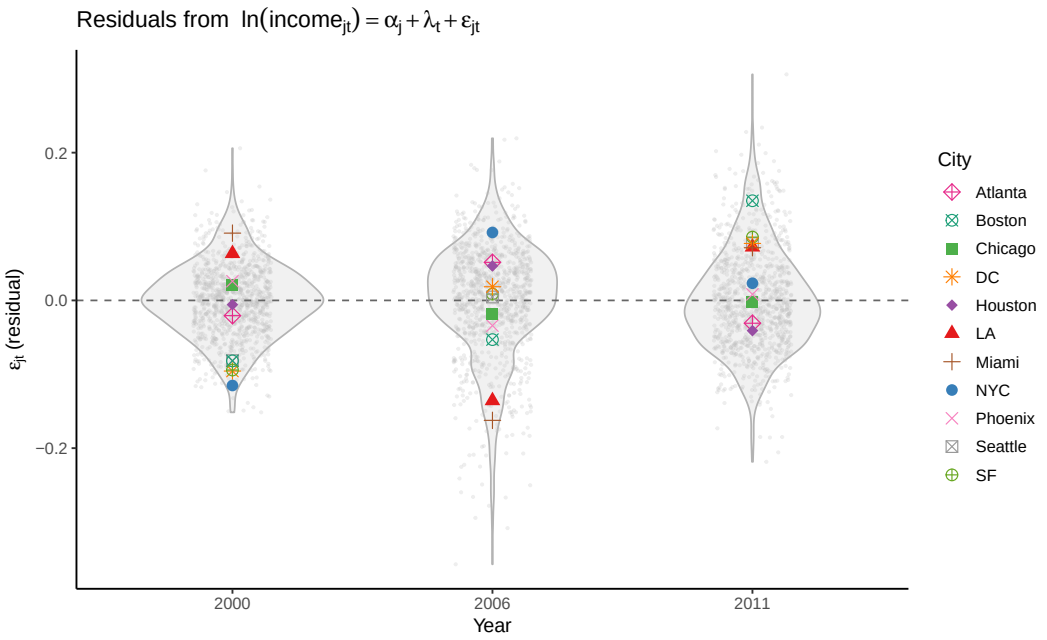


Figure F2: Distribution of residualized log housing-cost-adjusted income from $\ln(\widetilde{y}_{jt}) = \alpha_j + \lambda_t + \varepsilon_{jt}$. Violin plots show the residual distribution across `MIGPUMA`s by year; markers highlight selected metropolitan areas.

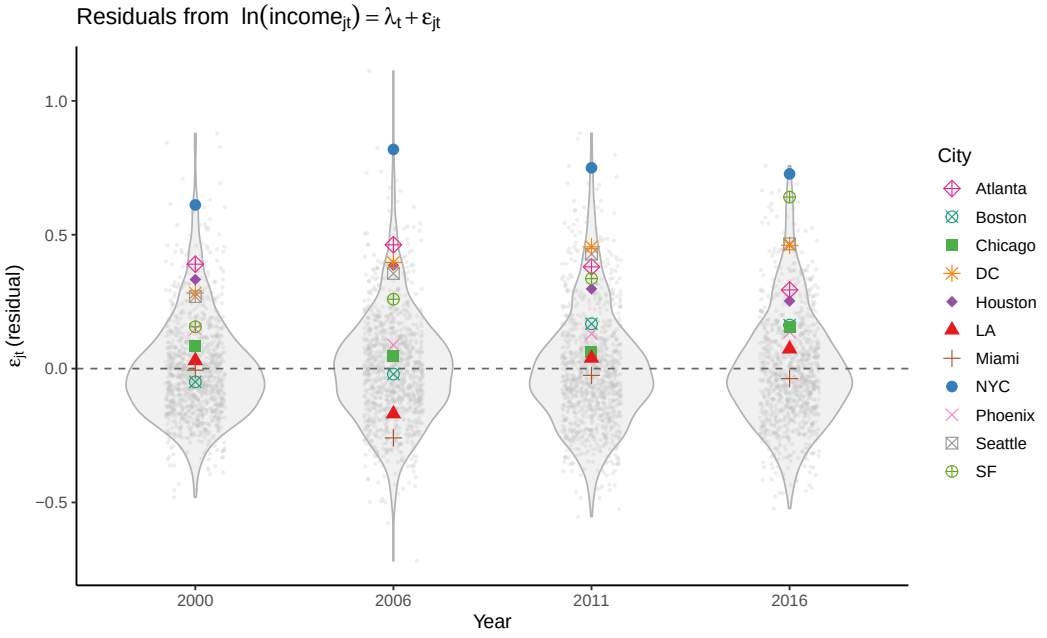


Figure F3: Distribution of residualized log housing-cost-adjusted income from $\ln(\widetilde{y}_{jt}) = \lambda_t + \eta_{jt}$ (year effects only).

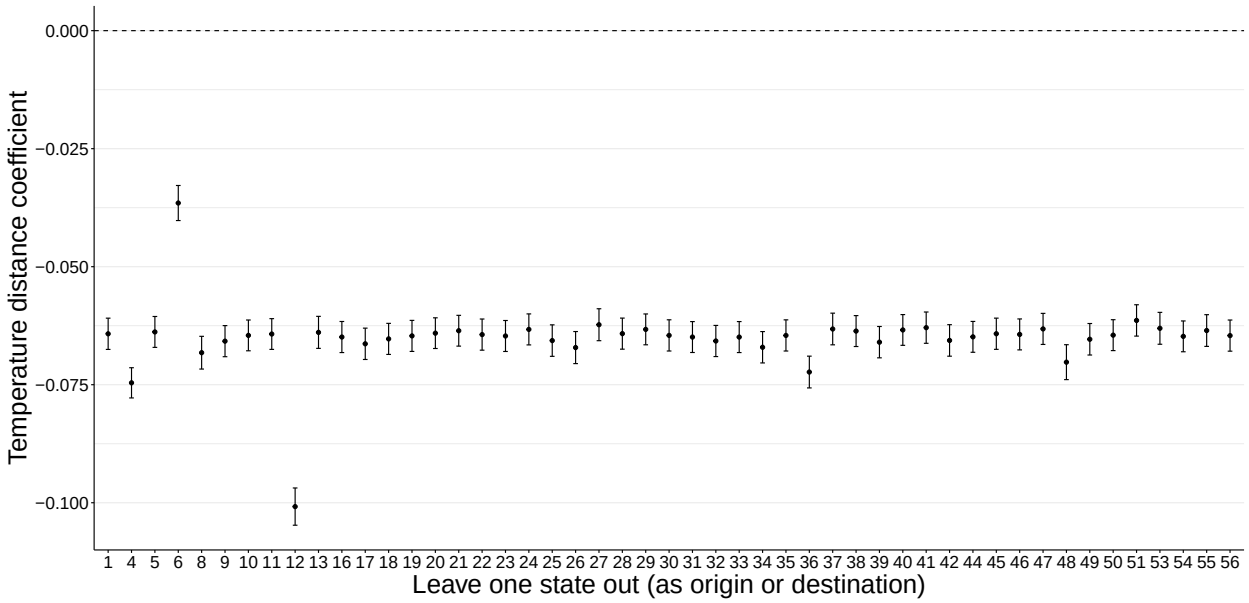
H Additional results

Table G1: PPML: Weighted bilateral flows. Stacked cross-section.

Dependent Variable:	Migration count		
Model:	(1)	(2)	(3)
Variables			
Temperature distance	-0.1308***	-0.0330***	-0.0488***
	(0.0039)	(0.0025)	(0.0021)
Precipitation distance	-0.0270***	-0.0044***	-0.0037***
	(0.0009)	(0.0005)	(0.0004)
Income (adj. housing costs)	1.565***	1.750***	0.3093***
	(0.0245)	(0.0243)	(0.0439)
Coastal distance (in km)		-0.0014***	-0.0014***
		(4.44×10^{-5})	(4.28×10^{-5})
Geographic distance (in km)		-0.0011***	-0.0009***
		(1.46×10^{-5})	(1.15×10^{-5})
Temperature			0.1218***
			(0.0023)
Total precipitation			-0.0159***
			(0.0004)
Age			-0.0109***
			(0.0031)
Male			6.011***
			(0.2109)
Married			-5.598***
			(0.2160)
Children			0.2129**
			(0.0924)
Farm			-10.05***
			(0.4590)
Black			-0.3201***
			(0.0651)
Hispanic			-0.5974***
			(0.0892)
Homeowner			-1.010***
			(0.1358)
College (compl.)			2.784***
			(0.0855)
Fixed-effects			
Origin-Year	Yes	Yes	Yes
Fit statistics			
WTP 1C	3,308.3	747.3	6,252.3
Temperature Difference (j-i) (mean)	0.000	0.000	0.000
Income (mean)	39,594.6	39,594.6	39,594.6
Migration count (mean)	7.855	7.855	7.855
Observations	4,017,570	4,017,570	4,017,570
Squared Correlation	0.12614	0.27977	0.37224
Pseudo R^2	0.29045	0.36930	0.43599
BIC	115,212,959.9	102,415,690.2	91,592,575.2

Clustered (Origin-Destination) standard-errors in parentheses
*Signif. Codes: ***: 0.01, **: 0.05, *: 0.1*

Figure G1: Leave one state out estimates of Temperature Distance



Notes: This figure plots estimates of the temperature distance coefficient from Equation (12) where each estimate represents the coefficient estimated in a sample where one state (in x-axis) is left out both as origin and destination. For a mapping FIPS state-code to state, see here. Bins indicate 95% confidence intervals with standard errors clustered at the origin-destination level.

Table G2: OLS: Weighted bilateral flows 2000-2016.

Dependent Variable:	log(Migrants/Stayers)		
Model:	(1)	(2)	(3)
Variables			
Temperature distance	-0.0438***	-0.0219***	-0.0220***
	(0.0006)	(0.0006)	(0.0006)
Precipitation distance	-0.0081***	-0.0018***	-0.0018***
	(0.0001)	(0.0001)	(0.0001)
Income (adj. housing costs)	0.2637***	0.3081***	0.3227***
	(0.0432)	(0.0439)	(0.0457)
Coastal distance (in km)		-0.0005***	-0.0005***
		(1.08×10^{-5})	(1.07×10^{-5})
Geographic distance (in km)		-0.0003***	-0.0003***
		(2.63×10^{-6})	(2.64×10^{-6})
Age			-0.0510***
			(0.0050)
Male			-3.365***
			(0.1674)
Married			1.279***
			(0.2251)
Children			-0.1659*
			(0.0901)
Farm			-3.493***
			(0.8209)
White			1.607***
			(0.4039)
Black			1.437***
			(0.4638)
hispan			-3.074***
			(0.4748)
Homeowner			-0.3015
			(0.2034)
College (compl.)			-0.9056***
			(0.2188)
Fixed-effects			
Year-Origin	Yes	Yes	Yes
Destination	Yes	Yes	Yes
Fit statistics			
WTP 1C	6,581.4	2,819.2	2,695.4
Income (mean)	39,594.6	39,594.6	39,594.6
Migration count (mean)	7.855	7.855	7.855
Observations	254,145	254,145	254,145
R^2	0.56915	0.59317	0.59510
Within R^2	0.06599	0.11806	0.12225

Clustered (Origin-Destination) standard-errors in parentheses
*Signif. Codes: ***: 0.01, **: 0.05, *: 0.1*

Table G3: PPML: Estimating semi-elasticities to distance measures.

Dependent Variable:	Migration count		
Model:	(1)	(2)	(3)
Variables			
log(Temperature distance)	-0.3295***	-0.0160***	-0.0160***
	(0.0046)	(0.0046)	(0.0046)
log(Precipitation distance)	-0.3603***	0.0036	0.0036
	(0.0044)	(0.0049)	(0.0049)
Income (adj. housing costs)	0.3158***	0.4138***	0.4905***
	(0.0641)	(0.0647)	(0.0646)
log(Geographic Distance)		-1.310***	-1.310***
		(0.0074)	(0.0074)
Age			-0.0773***
			(0.0073)
Male			-0.1207
			(0.2295)
Married			0.5228
			(0.3230)
Children			-0.3191***
			(0.1202)
Farm			-1.177
			(1.069)
Black			-0.0415
			(0.3346)
Hispanic			0.4649
			(0.3578)
Homeowner			-1.202***
			(0.2917)
College (compl.)			0.1536
			(0.3071)
Year-Origin	Yes	Yes	Yes
Destination	Yes	Yes	Yes
WTP 1C	35,365.8	1,309.4	1,103.2
Income (mean)	39,594.6	39,594.6	39,594.6
Migration count (mean)	7.855	7.855	7.855

Clustered (Origin-Destination) standard-errors in parentheses
*Signif. Codes: ***: 0.01, **: 0.05, *: 0.1*

Table G4: PPML: Alternative measures of temperature distance. 2000-2016.

Dependent Variable:	Migration count		
Model:	(1)	(2)	(3)
Variables			
Temperature distance	-0.0277***	-0.0762***	-0.0545***
	(0.0010)	(0.0035)	(0.0015)
Precipitation distance	-0.0089***	0.0022***	-0.0041***
	(0.0002)	(0.0002)	(0.0003)
Income (adj. housing costs)	0.4631***	0.4495***	0.4722***
	(0.0633)	(0.0633)	(0.0638)
Coastal distance (in km)	-0.0014***	-0.0017***	-0.0016***
	(2.94×10^{-5})	(2.79×10^{-5})	(2.95×10^{-5})
Geographic distance (in km)	-0.0009***	-0.0011***	-0.0009***
	(9.21×10^{-6})	(1.24×10^{-5})	(9.94×10^{-6})
Age	-0.0757***	-0.0739***	-0.0741***
	(0.0074)	(0.0074)	(0.0075)
Male	-0.1649	-0.1471	-0.1570
	(0.2291)	(0.2285)	(0.2292)
Married	0.6079*	0.6636**	0.5760*
	(0.3216)	(0.3217)	(0.3220)
Children	-0.3119***	-0.3406***	-0.3168***
	(0.1204)	(0.1207)	(0.1208)
Farm	-1.275	-1.355	-1.355
	(1.072)	(1.072)	(1.072)
Black	-0.0142	0.0619	0.0363
	(0.3366)	(0.3397)	(0.3389)
Hispanic	0.5144	0.4175	0.4057
	(0.3543)	(0.3471)	(0.3520)
Homeowner	-1.273***	-1.375***	-1.326***
	(0.2917)	(0.2871)	(0.2897)
College (compl.)	0.1549	0.2167	0.1503
	(0.3083)	(0.3067)	(0.3078)
Fixed-effects			
Year-Origin	Yes	Yes	Yes
Destination	Yes	Yes	Yes
Fit statistics			
Climate distance variables	January	July	Annual unweighted
WTP 1C	2,363.5	6,708.9	4,567.0
Income (mean)	39,594.6	39,594.6	39,594.6
Migration count (mean)	7.855	7.855	7.855
Observations	4,017,570	4,017,570	4,017,570
Squared Correlation	0.58399	0.57583	0.56372
Pseudo R^2	0.52540	0.51963	0.52043
BIC	77,113,925.1	78,049,583.2	77,919,094.6

Clustered (Origin-Destination) standard-errors in parentheses
*Signif. Codes: ***: 0.01, **: 0.05, *: 0.1*

Table G5: PPML: Alternative measure of income (controlling for housing costs). 2000-2016.

Dependent Variable:	Migration count		
Model:	(1)	(2)	(3)
Variables			
Temperature distance	-0.1372***	-0.0569***	-0.0568***
	(0.0020)	(0.0015)	(0.0015)
Precipitation distance	-0.0258***	-0.0047***	-0.0047***
	(0.0003)	(0.0003)	(0.0003)
Income	0.5166***	0.5256***	0.6287***
	(0.1119)	(0.1110)	(0.1208)
Housing cost	-0.1508***	-0.1417***	-0.2812***
	(0.0530)	(0.0522)	(0.0523)
Coastal distance (in km)		-0.0016***	-0.0016***
		(2.92×10^{-5})	(2.92×10^{-5})
Geographic distance (in km)		-0.0009***	-0.0009***
		(9.29×10^{-6})	(9.29×10^{-6})
Age			-0.0770***
			(0.0076)
Male			-0.0912
			(0.2317)
Married			0.6453**
			(0.3221)
Children			-0.3251***
			(0.1218)
Farm			-1.152
			(1.075)
Black			-0.0503
			(0.3422)
Hispanic			0.4105
			(0.3632)
Homeowner			-1.308***
			(0.3064)
College (compl.)			0.2437
			(0.3189)
Fixed-effects			
Year-Origin	Yes	Yes	Yes
Destination	Yes	Yes	Yes
Fit statistics			
WTP 1C	14,538.4	5,922.4	4,949.7
Temperature Difference (j-i) (mean)	0.000	0.000	0.000
Income (mean)	54,752.3	54,752.3	54,752.3
Migration count (mean)	7.855	7.855	7.855
Observations	4,017,570	4,017,570	4,017,570
Squared Correlation	0.45499	0.57016	0.57170
Pseudo R^2	0.45383	0.52026	0.52048
BIC	88,727,436.6	77,947,510.9	77,912,310.9

Clustered (Origin-Destination) standard-errors in parentheses
*Signif. Codes: ***: 0.01, **: 0.05, *: 0.1*

Table G6: Baseline results controlling for past networks.

Dependent Variable:	Migration count				
Model:	(1)	(2)	(3)	(4)	(5)
Variables					
Temperature distance	-0.0568***	-0.0562***	-0.0628***	-0.0636***	-0.0630***
	(0.0015)	(0.0027)	(0.0022)	(0.0022)	(0.0022)
Precipitation distance	-0.0047***	-0.0051***	-0.0056***	-0.0058***	-0.0056***
	(0.0003)	(0.0004)	(0.0003)	(0.0003)	(0.0003)
Income (adj. housing costs)	0.4744***	0.3869***	0.5877***	0.5826***	0.5883***
	(0.0641)	(0.0988)	(0.0725)	(0.0726)	(0.0725)
Coastal distance (in km)	-0.0016***	-0.0017***	-0.0017***	-0.0018***	-0.0017***
	(2.92×10^{-5})	(4.66×10^{-5})	(3.26×10^{-5})	(3.24×10^{-5})	(3.27×10^{-5})
Geographic distance (in km)	-0.0009***	-0.0009***	-0.0010***	-0.0011***	-0.0010***
	(9.29×10^{-6})	(1.56×10^{-5})	(1.27×10^{-5})	(1.24×10^{-5})	(1.27×10^{-5})
Age	-0.0741***	-0.0755***	-0.0799***	-0.0794***	-0.0798***
	(0.0075)	(0.0124)	(0.0079)	(0.0080)	(0.0080)
Male	-0.1675	-0.8442*	-0.4057	-0.4092	-0.4072
	(0.2291)	(0.5116)	(0.2633)	(0.2637)	(0.2632)
Married	0.5790*	1.216**	0.5930*	0.6030*	0.5928*
	(0.3220)	(0.4890)	(0.3554)	(0.3557)	(0.3554)
Children	-0.3146***	-0.5236**	-0.4389***	-0.4420***	-0.4386***
	(0.1209)	(0.2217)	(0.1358)	(0.1358)	(0.1358)
Farm	-1.361	0.3635	-1.070	-1.111	-1.069
	(1.072)	(1.813)	(1.190)	(1.190)	(1.190)
Black	0.0318	-3.273***	0.5205	0.5321	0.5199
	(0.3389)	(0.8101)	(0.3814)	(0.3814)	(0.3816)
Hispanic	0.4161	-1.215	-0.5561	-0.5405	-0.5570
	(0.3547)	(0.9501)	(0.3844)	(0.3859)	(0.3844)
Homeowner	-1.314***	-2.344***	-1.179***	-1.177***	-1.180***
	(0.2892)	(0.4777)	(0.3171)	(0.3175)	(0.3171)
College (compl.)	0.1383	1.650***	0.2798	0.2725	0.2787
	(0.3078)	(0.5448)	(0.3393)	(0.3394)	(0.3394)
Migration flows in previous census year		0.0435***			
		(0.0090)			
Migration flows in 1850-1940			0.1004***		
			(0.0077)		
Migration flows in 1850-1880				0.5379***	
				(0.0575)	
Migration flows in 1900-1940					0.1049***
					(0.0085)
Fixed-effects					
Year-Origin	Yes	Yes	Yes	Yes	Yes
Destination	Yes	Yes	Yes	Yes	Yes
Fit statistics					
Observations	4,017,570	2,047,876	2,801,536	2,801,536	2,801,536
Squared Correlation	0.57215	0.40943	0.58077	0.62668	0.57888
Pseudo R^2	0.52050	0.41164	0.55966	0.55887	0.55928
BIC	77,909,003.4	34,504,429.8	55,890,220.2	55,991,332.2	55,938,669.3

Clustered (Origin-Destination) standard-errors in parentheses
*Signif. Codes: ***: 0.01, **: 0.05, *: 0.1*

Table G7: PPML: Robustness dropping short moves. 2000-2016.

Dependent Variable:	Migration count		
Model:	(1)	(2)	(3)
Variables			
Temperature distance	-0.0493***	-0.0118***	-0.0200***
	(0.0015)	(0.0014)	(0.0016)
Precipitation distance	-0.0039***	-0.0012***	-0.0026***
	(0.0003)	(0.0002)	(0.0003)
Income (adj. housing costs)	0.4458***	0.4193***	0.4966***
	(0.0665)	(0.0778)	(0.0815)
Coastal distance (in km)	-0.0015***	-0.0009***	-0.0012***
	(2.78×10^{-5})	(2.3×10^{-5})	(2.97×10^{-5})
Geographic distance (in km)	-0.0009***	-0.0007***	-0.0007***
	(8.9×10^{-6})	(7.4×10^{-6})	(7.74×10^{-6})
Age	-0.0730***	-0.0673***	-0.0726***
	(0.0078)	(0.0087)	(0.0087)
Male	-0.0890	-0.2031	0.3171
	(0.2377)	(0.2779)	(0.2784)
Married	0.6267*	0.4599	0.2215
	(0.3333)	(0.3993)	(0.3912)
Children	-0.3197**	-0.2448*	-0.1474
	(0.1253)	(0.1464)	(0.1468)
Farm	-1.742	-0.0792	-0.1087
	(1.120)	(1.431)	(1.450)
Black	0.0628	-0.1651	-0.1873
	(0.3504)	(0.3902)	(0.3747)
Hispanic	0.5326	0.2495	-0.1354
	(0.3635)	(0.4092)	(0.4329)
Homeowner	-1.218***	-1.102***	-1.101***
	(0.2994)	(0.3492)	(0.3503)
College (compl.)	0.1061	-0.0008	-0.3535
	(0.3193)	(0.3822)	(0.3835)
Fixed-effects			
Year-Origin	Yes	Yes	Yes
Destination	Yes	Yes	Yes
Fit statistics			
Sample	Moves > 100km	Moves > 250km	Moves across states
WTP 1C	4,374.5	1,114.1	1,593.0
Income (mean)	39,594.6	39,594.6	39,594.6
Migration count (mean)	7.855	7.855	7.855
Observations	4,005,264	3,845,107	3,911,553

Clustered (Origin-Destination) standard-errors in parentheses
*Signif. Codes: ***: 0.01, **: 0.05, *: 0.1*

Table G8: Baseline results by tercile of origin temperature.

Dependent Variable:	Migration count		
Model:	(1)	(2)	(3)
Temperature distance	-0.0805***	-0.1539***	-0.3663***
	(0.0045)	(0.0060)	(0.0083)
Precipitation distance	-0.0057***	-0.0067***	0.0043***
	(0.0004)	(0.0005)	(0.0007)
Income (adj. housing costs)	0.4086***	0.5888***	0.1928
	(0.0939)	(0.1097)	(0.1194)
Coastal distance (in km)	-0.0018***	-0.0021***	-0.0015***
	(5.55×10^{-5})	(4.55×10^{-5})	(4.45×10^{-5})
Geographic distance (in km)	-0.0009***	-0.0008***	-0.0013***
	(1.42×10^{-5})	(1.36×10^{-5})	(1.93×10^{-5})
Origin temperature tercile	Hot	Middle	Cold
Year-Origin FE	Yes	Yes	Yes
Destination FE	Yes	Yes	Yes
Demographic controls	Yes	Yes	Yes
WTP 1C	7,797.6	10,349.1	75,236.9
Income (mean)	39,594.6	39,594.6	39,594.6
Migration count (mean)	7.855	7.855	7.855
Observations	1,320,040	1,323,103	1,302,454

Clustered (Origin-Destination) standard-errors in parentheses
*Signif. Codes: ***: 0.01, **: 0.05, *: 0.1*

Table G9: PPML: Weighted bilateral flows by tercile of origin temperature and direction of the move.

Dependent Variable:	Migration count					
Model:	(1)	(2)	(3)	(4)	(5)	(6)
Panel A: Contiguous U.S.						
Temperature distance	-0.1086***	0.0849***	-0.2085***	0.0934***	-0.1128***	-0.0435***
	(0.0228)	(0.0045)	(0.0082)	(0.0051)	(0.0054)	(0.0141)
Precipitation distance	0.0043**	-0.0072***	0.0036***	-0.0034***	-0.0025***	-0.0065***
	(0.0022)	(0.0008)	(0.0009)	(0.0007)	(0.0007)	(0.0010)
Income (adj. housing costs)	-0.4076**	0.0824	0.0246	-0.1366	0.4795***	1.324***
	(0.1643)	(0.0732)	(0.1261)	(0.0868)	(0.0868)	(0.1383)
Panel B: Excluding Sunbelt (Arizona, Florida, Texas)						
Temperature distance	-0.1098***	-0.0695***	-0.2134***	-0.0249***	-0.1523***	-0.1515***
	(0.0230)	(0.0070)	(0.0083)	(0.0075)	(0.0119)	(0.0260)
Precipitation distance	0.0039*	-0.0083***	0.0041***	-0.0049***	-0.0046***	-0.0086***
	(0.0022)	(0.0011)	(0.0009)	(0.0009)	(0.0011)	(0.0023)
Income (adj. housing costs)	-0.4253***	0.1588*	0.0379	-0.2689**	0.2439*	0.7541***
	(0.1649)	(0.0949)	(0.1279)	(0.1096)	(0.1315)	(0.2498)
Origin temperature tercile	Cold	Cold	Mild	Mild	Hot	Hot
Direction of the move	Hotter destination	Colder destination	Hotter destination	Colder destination	Hotter destination	Colder destination
Year-Origin FE	Yes	Yes	Yes	Yes	Yes	Yes
Controls	Yes	Yes	Yes	Yes	Yes	Yes
Observations	203,593	1,113,957	662,554	671,269	1,117,105	218,907

Clustered (Origin-Destination) standard-errors in parentheses
*Signif. Codes: ***: 0.01, **: 0.05, *: 0.1*

Table G10: PPML panel estimates using fold-level bilateral flows between 2000 and 2016.

Dependent Variable:	Number of migrants (per fold)		
Model:	(1)	(2)	(3)
Variables			
Temperature distance	-0.0757***	0.0089***	-0.0660***
	(0.0020)	(0.0026)	(0.0017)
Income (adj. housing costs)	0.2392***	0.3463***	0.3428***
	(0.0519)	(0.1001)	(0.0672)
Temperature distance × Male	0.0156***		
	(0.0018)		
Income × Male	0.0842		
	(0.0918)		
Temperature distance × Under age 65		-0.0853***	
		(0.0025)	
Income × Under age 65		-0.0659	
		(0.1148)	
Temperature distance × No College			0.0016
			(0.0020)
Income × No College			-0.1197
			(0.0900)
Socio-demographic controls	✓	✓	✓
Precipitation distance	✓	✓	✓
Geographic and travel distance	✓	✓	✓
Year-Origin-fold FE	Yes	Yes	Yes
Destination-fold FE	Yes	Yes	Yes
Fold	1="Female", 2="Male"	1="Age 65+", 2="Under 65"	1="College", 2="No College"
WTP 1C (1)	7,717.1	-811.0	10,032.9
WTP 1C (2)	9,306.0	11,093.0	6,770.8
Income (1)	24,389.0	31,681.0	52,139.0
Income (2)	50,079.0	40,675.0	23,464.0
Migration count (1)	3.095	0.732	5.056
Migration count (2)	4.760	7.123	2.799
Observations	7,999,738	7,489,473	7,950,980

Clustered (Origin-Destination) standard-errors in parentheses
*Signif. Codes: ***: 0.01, **: 0.05, *: 0.1*

Table G11: PPML: Ethnicity-level bilateral flows with interactions.

Dependent Variable:	Number of migrants
Model:	(1)
Variables	
Temperature distance	-0.0864***
	(0.0067)
Income (adj. housing costs)	0.6102***
	(0.0273)
Temperature distance × fold = Black	-0.1596***
	(0.0112)
Temperature distance × fold = Hispanic	-0.0437***
	(0.0087)
Temperature distance × fold = White	-0.0183***
	(0.0063)
Income (adj. housing costs) × fold = Black	-0.2115***
	(0.0328)
Income (adj. housing costs) × fold = Hispanic	-0.5543***
	(0.0302)
Income (adj. housing costs) × fold = White	0.1917***
	(0.0324)
Socio-demographic controls	✓
Precipitation distance	✓
Geographic and travel distance	✓
Year-Origin-fold FE	Yes
Destination-fold FE	Yes
Migration count (Black)	0.82
Migration count (Hispanic)	0.69
Migration count (White)	5.78
Migration count (Other)	0.56
Income (Black)	27,246
Income (Hispanic)	26,959
Income (White)	39,182
Income (Other)	36,460
WTP 1°C (Black)	16,426
WTP 1°C (Hispanic)	58,858
WTP 1°C (White)	5,637
WTP 1°C (Other)	5,902
Observations	14,915,748

Clustered (Origin-Destination) standard errors in parentheses
*Signif. Codes: ***: 0.01, **: 0.05, *: 0.1*